



The 1997 spectroscopic GEISA databank

N. Jacquinet-Husson^{a,*}, E. Arié^b, J. Ballard^c, A. Barbe^d, G. Bjoraker^e, B. Bonnet^a,
L. R. Brown^f, C. Camy-Peyret^g, J.P. Champion^h, A. Chédin^a, A. Chursinⁱ,
C. Clerbaux^{j,1}, G. Duxbury^k, J.-M. Flaud^l, N. Fourrié^a, A. Fayt^m, G. Graner^b,
R. Gamacheⁿ, A. Goldman^o, Vl. Golovkoⁱ, G. Guelachvili^b, J.M. Hartmann^b,
J.C. Hilico^h, J. Hillman^f, G. Lefèvre^a, E. Lellouch^p, S.N. Mikhaïlenkoⁱ,
O.V. Naumenkoⁱ, V. Nemtchinov^q, D.A. Newnham^c, A. Nikitinⁱ, J. Orphal^r,
A. Perrin^l, D.C. Reuter^f, C.P. Rinsland^s, L. Rosenmann^t, L.S. Rothman^u,
N.A. Scott^a, J. Selby^v, L.N. Sinitzaⁱ, J.M. Sirota^f, A.M. Smith^w, K.M. Smith^c,
Vl. G. Tyuterev^d, R.H. Tipping^x, S. Urban^y, P. Varanasi^q, M. Weber^r

^aLaboratoire de Météorologie Dynamique du CNRS, Ecole Polytechnique, 91128 Palaiseau, France

^bLaboratoire de Physique Moléculaire et Applications, CNRS, Bât.350, Université Paris-Sud, Campus d'Orsay, France

^cRutherford Appleton Laboratory, Chilton, Didcot, Oxon, OX11 0QX, UK

^dGroupe de Spectrométrie Moléculaire et Atmosphérique, Associé au CNRS, Faculté des Sciences, Reims, France

^eLaboratory for Extraterrestrial Physics, NASA Goddard Space Flight Center, Greenbelt, MD 20771, USA

^fJet Propulsion Laboratory, California Institute of Technology, Pasadena, CA 91109, USA

^gLaboratoire de Physique Moléculaire et Applications, CNRS, Université Pierre et Marie Curie, Paris, France

^hLaboratoire de Physique de l'Université de Bourgogne, Associé au CNRS, Dijon, France

ⁱInstitute of Atmospheric Optics, Tomsk, Russia

^jLaboratoire de Chimie Physique Moléculaire, Université Libre de Bruxelles, Bruxelles, Belgium

^kDepartment of Physics and Applied Physics, University of Strathclyde, Glasgow, G4 0NG, UK

^lLaboratoire de Photophysique Moléculaire, CNRS, Bât.210, Université Paris Sud, Campus d'Orsay, France

^mLaboratoire de Spectroscopie Moléculaire, Université Catholique de Louvain, Louvain-la-Neuve, Belgium

ⁿDepartment of Environmental, Earth and Atmospheric Sciences, University of Massachusetts Lowell, Lowell, MA 01854, USA

^oDepartment of Physics, University of Denver, Denver, CO 80208, USA

^pDESPA, Observatoire de Paris (Section de Meudon), Meudon, France

^qInstitute for Terrestrial and Planetary Atmospheres, Marine Sciences Research Center, State University of New York at Stony Brook, Stony Brook, NY 11794-5000, USA

^rInstitute of Environmental Physics/Institute of Remote Sensing, University of Bremen, D-28334 Bremen, Germany

^sNASA Langley Research Center, Atmospheric Sciences Division, Hampton, VA 23665, USA

* Corresponding author. Tel.: 00 33 1 69 33 48 02; Fax: 00 33 1 69 33 30 05; E-mail: husson@ara01.polytechnique.fr

¹ Now at Service d'Aéronomie du CNRS, Université Pierre et Marie Curie, Paris, France.

¹*Laboratoire d'Énergétique Moléculaire et Macroscopique Combustion, CNRS et Ecole Centrale de Paris, Châtenay-Malabry, France*

²*AF Geophysics Directorate, Hanscom AFB, Hanscom, MA 01731, USA*

³*Northrop Grumman, Bethpage, Long Island, NY 11714, USA*

⁴*Institute for Physical and Theoretical Chemistry of the Technical University of Munich, D-8046 Garching, Germany*

⁵*Department of Physics and Astronomy, University of Alabama, Tuscaloosa, AL 35487, USA*

⁶*J. Heyrovsky Institute of Physical Chemistry and Electrochemistry, Prague, Czech Republic*

Received 9 April 1998

Abstract

The current version GEISA-97 of the computer-accessible database system GEISA (Gestion et Etude des Informations Spectroscopiques Atmosphériques: Management and Study of Atmospheric Spectroscopic Information) is described. This catalogue contains 1,346,266 entries. These are spectroscopic parameters required to describe adequately the individual spectral lines belonging to 42 molecules (96 isotopic species) and located between 0 and 22,656 cm^{-1} . The featured molecules are of interest in studies of the terrestrial as well as the other planetary atmospheres, especially those of the Giant Planets. GEISA-97 contains also a catalog of absorption cross-sections of molecules such as chlorofluorocarbons which exhibit unresolvable spectra. The modifications and improvements made to the earlier edition (GEISA-92) and the data management software are described. GEISA-97 and the associated management software are accessible from the ARA/LMD (Laboratoire de Météorologie Dynamique du CNRS, France) web site: <http://ara01.polytechnique.fr/registration>. © 1999 Elsevier Science Ltd. All rights reserved.

1. Introduction

Adequate tools are required to perform reliable radiative transfer calculations to meet the needs of communities involved in understanding the atmospheres of the Earth and other planets. In particular, accurate spectral analyses of Earth or planetary spectra observed by new generations of high spectral resolution vertical atmospheric sounders [1, 2] will result in an improved knowledge of their atmospheric and surface properties. The performance of instruments like AIRS [1] (Atmospheric Infrared Sounder) in the U.S.A, and IASI [2] (Infrared Atmospheric Sounding Interferometer) in Europe, which have a better vertical resolution and accuracy compared to the presently existing satellite infrared temperature sounders, is directly related to the quality of the spectroscopic parameters of the optically active atmospheric gases since these are essential input in the forward models used to simulate recorded radiance spectra. The ARA (Atmospheric Radiation Analysis) group at LMD (Laboratoire de Météorologie Dynamique du CNRS, France) developed the GEISA (Gestion et Etude des Informations Spectroscopiques Atmosphériques: Management and Study of Atmospheric Spectroscopic Information) computer accessible database system [3–5], in 1974. This early effort implemented the so-called “line-by-line and layer-by-layer” approach for forward radiative transfer modeling action. This activity is of interest to research groups involved in direct and inverse radiative transfer studies.

The role of molecular spectroscopy in modern atmospheric research has entered a new phase with the advent of highly sophisticated spectroscopic instruments and computers. Retrieval of the concentrations of radiatively active molecular species from observed spectra of planetary atmospheres using available spectroscopic databases and atmospheric models has become fairly routine.

The molecular spectroscopist is constantly on demand to deliver data that are not only appropriate but essential for the analyses of the planetary atmospheric observations. GEISA is dedicated to meeting that aim.

Currently, GEISA is involved in activities, with the purpose of assessing the IASI (Infrared Atmospheric Sounding Interferometer) measurements capabilities and its own database quality, within the ISSWG (IASI Sounding Working Group), in the frame of the CNES (Centre National d'Etudes Spatiales, France)/EUMETSAT (European organization for the exploitation of METeorological SATellites) European Polar System (EPS), by simulating high resolution radiances and/or using experimental data, as described in Ref. [6].

2. Overview of the 1997 edition of the GEISA spectroscopic database

The 1997 version of the GEISA database (hereafter referred to as GEISA-97) contains line parameters for 42 molecules (96 isotopic species) with 1 346 266 entries between 0 and 22 656 cm^{-1} . It has molecules of interest for both terrestrial and other planetary atmospheres (for example, C_2H_4 , GeH_4 , C_3H_8 , C_2N_2 , C_4H_2 , HC_3N , H_2S , HCOOH and C_3H_4 , for the Giant Planets). GEISA-97 has been developed in close cooperation with the contributors of three spectroscopic databases: ATMOS-95 (Atmospheric Trace Molecule Spectroscopy) [7], HITRAN-96 (High resolution TRANsmission) [8] and TDS (Tomsk Dijon Spectroscopic project; Traitement des Données Spectroscopiques)/STDS (Spherical Top Data System) [9, 10].

Since the release of the former edition [4, 5] in 1992 (hereafter referred to as GEISA-92), two new species, HO_2 and ClONO_2 (formerly only present in the cross-sections file of GEISA-92), have been added for the first time, and 17 existing molecules: O_3 , N_2O , CH_4 , NO , SO_2 , NO_2 , NH_3 , HNO_3 , OH , ClO , OCS , $^{13}\text{C}^{12}\text{CH}_6$, CH_3D , C_2H_2 , C_2H_4 , H_2O_2 , H_2S , have been updated for GEISA-97. These changes have added 10 new isotopes: three for the new molecules and seven for the already existing molecules (two in O_3 , one in CO , two in OCS , one in C_2H_6 , and one in C_2H_4) and the parameters of 19 species have been updated or included. Finally, in addition to the individual lines spectroscopic data catalog, GEISA-97 also has a catalog of cross-sections at different temperatures and pressures for species (such as chlorofluorocarbons) with complex spectra that are too dense for discrete parameterization. The GEISA-97 cross-sections file and its associated management software are described later (in Section 4).

The detailed summary of the line parameters in GEISA-97 is provided in Table 1. The items listed for each molecular species, given in column 1, are: the identification code (ID codes defined for the GEISA management software in Ref. [11]), the number of lines, the intensity average, the mean halfwidth at half maximum, the identification codes of its various isotopes, and for each isotope: the number of lines, the transitions minimum and maximum wavenumbers (in cm^{-1}), and the lines intensities minimum and maximum values (in cm molecule^{-1}), in columns 2–11, respectively.

In Table 2, the various isotopes chemical formula corresponding to the GEISA-97 molecular and isotopic codes are provided.

The format fields for each transition are the same as in the previous editions [4, 6] and the fields are shown and defined in Table 3. The A–J fields are those used in the GEISA management associated softwares [4, 5, 11], as follows: (A) wavenumber (cm^{-1}) of the line associated with the rovibrational transition; (B) intensity of the line (cm molecule^{-1} at 296 K); (C) Lorentzian collision

Table 1
Detailed content of GEISA-97 edition

Mol.	ID	# Lines	Intensity average	Alpha average	Iso. ID	# Lines	F-Min (cm ⁻¹)	F-Max (cm ⁻¹)	Int-Min (cm molec ⁻¹)	Int-Max (cm molec ⁻¹)
H ₂ O	1	50217	1.450E-21	0.069	161	30117	0.401	22656.465	1.010E-32	2.670E-18
					162	9799	0.007	5507.548	1.240E-32	2.700E-22
					171	3744	6.471	11150.790	1.490E-27	9.830E-22
					181	6357	6.785	13900.421	1.000E-27	5.390E-21
					182	200	1231.680	1607.611	1.000E-26	7.940E-26
CO ₂	2	62816	1.793E-21	0.071	626	27896	442.006	9648.007	0.000E+00 (§)	3.520E-18
					636	9154	497.201	8104.666	0.000E+00 (§)	3.570E-20
					628	13554	507.860	8132.007	1.390E-36	6.850E-21
					627	6625	554.909	6961.226	1.000E-27	1.280E-21
					638	2312	567.596	4946.384	3.700E-27	7.230E-23
					637	1584	584.754	3641.072	3.710E-27	1.360E-23
					828	1107	615.974	3669.609	1.760E-40	1.310E-23
					728	288	626.438	2358.226	3.870E-27	2.500E-24
					838	296	2115.685	2276.481	4.870E-42	1.760E-25
					O ₃	3	281607	6.533E-23	0.069	666
668	19147	0.921	1177.493	4.880E-28						7.760E-23
686	7513	1.177	1145.690	7.500E-28						7.560E-23
667	58254	0.289	820.380	5.340E-31						5.570E-25
676	28938	0.213	822.795	1.490E-31						6.060E-25
N ₂ O	4	26771	2.688E-21	0.075	446	19423	0.838	5131.249	4.000E-27	1.000E-18
					447	1004	542.242	3482.917	3.430E-26	4.150E-22
					448	2034	545.179	3463.967	1.230E-25	2.050E-21
					456	2128	5.028	3462.689	5.220E-26	3.670E-21
					546	2182	4.858	3473.528	4.720E-26	3.600E-21
CO	5	13515	7.545E-22	0.047	26	5908	3.530	8464.883	7.880E-78	4.460E-19
					27	748	3.714	6338.061	8.190E-40	1.600E-22
					28	770	3.629	6266.578	7.610E-39	8.320E-22
					36	4768	3.414	8180.219	3.610E-73	4.680E-21
					38	741	3.462	6123.294	2.580E-40	8.700E-24
					37	580	1807.871	6196.551	1.030E-36	1.680E-24
CH ₄	6	66883	2.622E-22	0.052	211	56989	0.010	6184.492	4.060E-34	2.062E-19
					311	9894	0.032	6069.086	4.100E-34	2.329E-21
O ₂	7	6292	4.117E-26	0.044	66	1435	0.000	15927.806	0.000E+00 (§)	8.833E-24
					67	4186	0.000	14536.515	1.147E-47	5.337E-26
					68	671	1.572	15851.213	1.186E-35	1.710E-26
NO	8	94738	4.989E-23	0.053	46	93360	0.000	9273.214	1.401E-85	6.211E-20
					48	679	1601.909	2038.846	4.190E-28	1.390E-22
					56	699	1609.585	2060.462	4.430E-28	2.550E-22
SO ₂	9	38853	1.065E-21	0.114	626	38566	0.017	4092.948	1.020E-28	6.090E-20
					646	287	2463.470	2496.088	9.740E-24	3.430E-23
NO ₂	10	100680	6.194E-22	0.067	646	100680	0.498	2938.381	4.240E-28	1.300E-19
NH ₃	11	11152	4.275E-21	0.077	411	10062	0.215	5294.501	2.970E-29	5.450E-19
					511	1090	0.375	5179.786	5.460E-29	1.990E-21
PH ₃	12	4635	6.457E-21	0.075	131	4635	17.805	2445.553	3.690E-28	2.930E-19
HNO ₃	13	171504	6.879E-22	0.105	146	171504	0.035	1769.982	3.490E-27	3.020E-20
OH	14	41786	1.048E-21	0.044	61	41631	0.005	19267.869	1.401E-85	3.458E-18
					62	90	0.010	1.824	2.090E-31	5.780E-29
					81	65	0.053	6.325	1.200E-30	1.200E-26
HF	15	107	6.772E-19	0.041	19	107	41.111	11535.570	1.100E-26	1.440E-17
HCl	16	533	3.189E-20	0.040	15	284	20.270	13457.841	1.090E-26	5.030E-19
					17	249	20.240	10994.721	1.010E-26	1.610E-19
HBr	17	576	1.072E-20	0.051	19	289	16.237	9758.564	1.000E-26	1.210E-19
					11	287	16.232	9757.189	1.010E-26	1.180E-19
HI	18	237	4.623E-21	0.050	17	237	12.509	8487.305	1.020E-26	1.540E-19

Table 1
Continued

Mol.	ID	# Lines	Intensity average	Alpha average	Iso. ID	# Lines	F-Min (cm ⁻¹)	F-Max (cm ⁻¹)	Int-Min (cm molec ⁻¹)	Int-Max (cm molec ⁻¹)
<u>ClO</u>	19	7230	1.605E-22	0.087	56 76	3599 3631	0.028 0.015	1207.639 1199.840	1.520E-29 5.090E-30	3.240E-21 1.030E-21
<u>OCS</u>	20	24922	4.251E-21	0.090	622 624 632 623 822 634	14500 4764 2403 1802 1096 357	0.406 0.396 0.404 509.007 0.381 1972.188	4118.004 4115.931 4012.468 4115.588 4041.565 2910.543	1.560E-25 6.400E-27 1.720E-27 1.010E-23 2.620E-28 1.010E-23	8.550E-20 4.720E-20 1.200E-20 8.430E-21 2.090E-21 5.240E-22
H ₂ CO	21	2702	8.610E-21	0.120	126 128 136	1772 367 563	0.000 0.035 0.037	2998.527 47.486 75.745	1.020E-38 1.160E-30 2.020E-30	7.500E-20 1.110E-22 6.290E-22
<u>C₂H₆</u>	22	14981	2.686E-22	0.101	226 236	8944 6037	765.027 725.603	3000.486 918.717	5.800E-27 1.320E-28	3.210E-20 1.770E-23
<u>CH₃D</u>	23	11524	9.333E-25	0.060	212	11524	7.760	3146.460	5.570E-30	4.030E-22
<u>C₂H₂</u>	24	1668	2.340E-20	0.061	211 231	1432 236	604.774 613.536	3358.285 3374.223	1.370E-27 3.820E-26	1.080E-18 1.580E-20
<u>C₂H₄</u>	25	12978	1.411E-21	0.087	211 311	12967 281	701.203 2947.832	3242.172 3180.238	6.940E-26 5.060E-24	8.410E-20 1.620E-21
GeH ₄	26	824	4.978E-20	0.100	824	804	1937.371	2224.570	1.960E-22	3.680E-19
HCN	27	2575	1.205E-20	0.132	124 125 134	2275 115 185	2.956 2.870 2.880	18407.973 9671.953 9627.961	1.780E-28 5.110E-26 4.150E-26	7.100E-19 2.730E-21 8.290E-21
C ₃ H ₈	28	9019	4.168E-23	0.080	221	9019	700.015	799.930	3.770E-24	4.310E-22
C ₂ N ₂	29	2577	2.668E-21	0.080	224	2577	203.955	2181.690	6.590E-24	2.580E-20
C ₄ H ₂	30	1405	3.445E-21	0.100	211	1405	190.588	654.425	2.650E-24	6.930E-20
HC ₃ N	31	2027	2.693E-21	0.100	124	2027	474.293	690.860	6.360E-24	4.420E-20
HOCl	32	15565	2.295E-21	0.060	165 167	8057 7508	0.024 0.349	3799.249 3799.682	1.650E-27 7.220E-28	3.590E-20 1.140E-20
N ₂	33	117	5.729E-29	0.047	44	117	2001.711	2619.230	2.330E-34	3.410E-28
CH ₃ Cl	34	9355	5.584E-22	0.085	215 217	5311 4044	679.050 674.143	3172.927 3161.830	1.250E-25 4.190E-26	1.130E-20 3.540E-21
H ₂ O ₂	35	100781	5.090E-22	0.107	166	100781	0.043	1499.487	5.090E-29	5.610E-20
<u>H₂S</u>	36	20788	2.992E-22	0.136	121 131 141	12330 3564 4894	2.985 5.601 5.615	4256.547 4098.234 4171.176	1.450E-26 2.020E-26 2.020E-26	1.360E-19 5.990E-21 1.080E-21
HCOO H	37	3388	5.186E-21	0.400	261	3388	1060.962	1161.251	2.140E-22	2.840E-20
COF ₂	38	54866	2.178E-21	0.084	269	54866	725.005	1981.273	4.740E-24	3.830E-20
SF ₆	39	11520	4.551E-21	0.050	236	11520	940.425	952.238	2.160E-22	1.500E-20
C ₃ H ₄	40	3390	4.277E-22	(*)	341	3390	290.274	359.995	2.020E-23	3.180E-21
HO ₂	41	26963	9.907E-22	0.088	166	26963	0.055	3675.819	3.550E-27	2.900E-20
<u>ClONO₂</u>	42	32199	1.093E-22	0.140	564 764	21988 10211	763.641 765.212	797.741 790.805	1.250E-24 6.340E-25	3.850E-22 1.260E-22
TOTAL LINES IN GEISA 1997: 1,346,266										

Underlined molecules are new or updated for GEISA-97. (*) missing value set to 0.000. (§) minimum intensity value corresponding to extremely weak line

halfwidth (cm⁻¹ atm⁻¹ at 296 K); (D) energy of the lower level of the transition (cm⁻¹); (E) transition quantum identifications for the lower and upper levels of the transition; (F) temperature-dependent coefficient *n* of the halfwidth (when *n* is not available, its value is set to zero); (G) identification code for isotope; (I) identification code for molecule; (J) internal code for GEISA

Table 2
Summary of molecule and isotope codes in GEISA-97

Molecule	Molecule Code	Isotope Code	Formula
H ₂ O	1	161	H ¹⁶ OH
		162	H ¹⁶ OD
		171	H ¹⁷ OH
		181	H ¹⁸ OH
		182	H ¹⁸ OD
CO ₂	2	626	¹⁶ O ¹² C ¹⁶ O
		627	¹⁶ O ¹² C ¹⁷ O
		628	¹⁶ O ¹² C ¹⁸ O
		636	¹⁶ O ¹³ C ¹⁶ O
		637	¹⁶ O ¹³ C ¹⁷ O
		638	¹⁶ O ¹³ C ¹⁸ O
		728	¹⁷ O ¹² C ¹⁸ O
		828	¹⁸ O ¹² C ¹⁸ O
		838	¹⁸ O ¹³ C ¹⁸ O
O ₃	3	666	¹⁶ O ¹⁶ O ¹⁶ O
		668	¹⁶ O ¹⁶ O ¹⁸ O
		686	¹⁶ O ¹⁸ O ¹⁶ O
		667	¹⁶ O ¹⁶ O ¹⁷ O
		676	¹⁶ O ¹⁷ O ¹⁶ O
N ₂ O	4	446	¹⁴ N ¹⁴ N ¹⁶ O
		447	¹⁴ N ¹⁴ N ¹⁷ O
		448	¹⁴ N ¹⁴ N ¹⁸ O
		456	¹⁴ N ¹⁵ N ¹⁶ O
		546	¹⁵ N ¹⁴ N ¹⁶ O
CO	5	26	¹² C ¹⁶ O
		27	¹² C ¹⁷ O
		28	¹² C ¹⁸ O
		36	¹³ C ¹⁶ O
		37	¹³ C ¹⁷ O
		38	¹³ C ¹⁸ O
CH ₄	6	211	¹² CH ₄
		311	¹³ CH ₄
O ₂	7	66	¹⁶ O ¹⁶ O
		67	¹⁶ O ¹⁷ O
		68	¹⁶ O ¹⁸ O
NO	8	46	¹⁴ N ¹⁶ O
		48	¹⁴ N ¹⁸ O
		56	¹⁵ N ¹⁶ O
SO ₂	9	626	³² S ¹⁶ O ₂
		646	³⁴ S ¹⁶ O ₂
NO ₂	10	646	¹⁴ N ¹⁶ O ₂
NH ₃	11	411	¹⁴ NH ₃
		511	¹⁵ NH ₃

Table 2
Continued

Molecule	Molecule Code	Isotope Code	Formula
PH ₃	12	131	³¹ P H ₃
HNO ₃	13	146	H ¹⁴ N ¹⁶ O
OH	14	61	¹⁶ O H
		62	¹⁶ O D
		81	¹⁸ O H
HF	15	19	H ¹⁹ F
HCl	16	15	H ³⁵ Cl
		17	H ³⁷ Cl
HBr	17	11	H ⁸¹ Br
		19	H ⁷⁹ Br
HI	18	17	H ¹²⁷ I
ClO	19	56	³⁵ Cl ¹⁶ O
		76	³⁷ Cl ¹⁶ O
OCS	20	622	¹⁶ O ¹² C ³² S
		623	¹⁶ O ¹² C ³³ S
		624	¹⁶ O ¹² C ³⁴ S
		632	¹⁶ O ¹³ C ³² S
		634	¹⁶ O ¹³ C ³⁴ S
		722	¹⁷ O ¹² C ³² S
		822	¹⁸ O ¹² C ³² S
H ₂ CO	21	126	H ₂ ¹² C ¹⁶ O
		128	H ₂ ¹² C ¹⁸ O
		136	H ₂ ¹³ C ¹⁶ O
C ₂ H ₆	22	226	¹² C ₂ H ₆
		236	¹² C ¹³ C H ₆
CH ₃ D	23	212	¹² CH ₃ D
C ₂ H ₂	24	221	¹² C ₂ H ₂
		231	¹² C ¹³ C H ₂
C ₂ H ₄	25	211	¹² C ₂ H ₄
		311	¹² C ¹³ C H ₄
GeH ₄	26	411	⁷⁴ GeH ₄
HCN	27	124	H ¹² C ¹⁴ N
		125	H ¹³ C ¹⁵ N
		134	H ¹³ C ¹⁴ N
C ₃ H ₈	28	221	¹² C ₃ H ₈
C ₂ N ₂	29	224	¹² C ₂ ¹⁴ N ₂
C ₄ H ₂	30	211	¹² C ₄ H ₂
HC ₃ N	31	124	H ¹² C ₃ ¹⁴ N
HOCl	32	165	H ¹⁶ O ³⁵ Cl
		167	H ¹⁶ O ³⁷ Cl
N ₂	33	44	¹⁴ N ¹⁴ N

Table 2
Continued

Molecule	Molecule Code	Isotope Code	Formula
CH ₃ Cl	34	215	¹² CH ₃ ³⁵ Cl
		217	¹² CH ₃ ³⁷ Cl
H ₂ O ₂	35	166	H ₂ ¹⁶ O ¹⁶ O
H ₂ S	36	121	H ₂ ³² S
		131	H ₂ ³³ S
		141	H ₂ ³⁴ S
HCOOH	37	261	H ¹² C ¹⁶ O ¹⁶ OH
COF ₂	38	269	¹² C ¹⁶ O ¹⁹ F ₂
SF ₆	39	29	³² S ¹⁹ F ₆
C ₃ H ₄	40	341	¹² C ₃ H ₆
HO ₂	41	166	H ¹⁶ O ₂
ClONO ₂	42	564	¹⁵ Cl ¹⁶ O ¹⁴ N ¹⁶ O ₂
		764	¹⁷ Cl ¹⁶ O ¹⁴ N ¹⁶ O ₂

data identification. The K–Q fields correspond to information related to the actual transition, to allow comparison with other databases using the HITRAN format [12]. These fields, not of prime importance for the GEISA related software, correspond respectively to the following parameters: (K) molecule number; (L) isotope number (1—most abundant; 2—second, ...); (M) transition probability (Debye); (N) self-broadened halfwidth (HWHM) (cm⁻¹ atm⁻¹ at 296 K); (O) air-broadened pressure shift of line transition (cm⁻¹ atm⁻¹); (P) accuracy indices for frequency, intensity and halfwidths; (Q) indices of references for frequency, intensity and halfwidth. A blank field corresponds to a missing information.

The contents of the GEISA-97 and HITRAN-96 databases are compared in Tables 4 and 5. The molecular species cataloged in the line parameters portion of GEISA-97 and HITRAN-96 are given in Table 4. The molecular species formula are listed in column 1 and their identification codes for database management in column 2, where GEISA-97 is referred to as “G” and HITRAN-96 as “H”. For each molecular species, the numbers of bands, isotopes and lines, are given in columns 3, 4 and 5, respectively, for both databases. The minimum and maximum spectral ranges (in cm⁻¹) corresponding to the GEISA-97 transitions are in columns 6 and 7, respectively.

For the molecules commonly used in GEISA-97 and HITRAN-96, the differences between the two databases are highlighted in Table 5 for: line positions ν , in column 3, intensities I , in column 4, halfwidths at half maximum γ , in column 5. The molecular species are listed in column 1, and the spectral region in column 2. The related references are given in the last column.

3. Alterations to molecular line parameters for GEISA-97 edition

3.1. O₃ (molecule 3)

Compared to the previous version of GEISA, the present update involves the 17-species of ozone (¹⁶O¹⁷O¹⁶O and ¹⁷O¹⁶O¹⁶O) for the microwave and 17 μ m regions and for the ¹⁶O₃ main

Table 3
Fields of the format for each transition in the GEISA database

Fortran Format Descriptor	F10.6	D10.3	F5.3	F10.3	A36	F4.2	I4	I3	A3	I2	I1	E10.3	F5.4	F8.6	I3	I6	120 characters
C % Format Descriptor	10.6f	10.3e	5.3f	10.3f	.36s	4.2f	4i	3i	.3s	2i	1i	10.3e	5.4f	8.6f	3i	6i	
Fortran Variable Type ¹	R*4	R*8	R*4	R*4	C*36	R*4	I*4	I*4	C*4	I*4	I*4	R*4	R*4	R*4	I*4	I*4	100 bytes
C Variable Type ²	F	D	F	D	C[36]	F	I	I	C[4]	I	I	F	F	F	I	I	
Byte internal Storage ³	4	8	4	4	36	4	4	4	4	4	4	4	4	4	4	4	
Field Name ^{4,5}	A	B	C	D	E	F	G	I	J	K	L	M	N	O	P	Q	16 fields

- (1) The R, I, C symbols are abbreviations for the conventional Real, Integer and Character Fortran type declarators.
- (2) The F, D, I, C symbols are abbreviations for the standard float, double, integer and char C type declarators.
- (3) Real type values (Fortran R* or C F, D) are stored in IEEE format.
- (4) Character strings (E and J fields) are blank right justified (no ending null character).
The A-J fields are those used in the GEISA software:
 - (A) Wavenumber (cm⁻¹) of the line associated with the vibro-rotational transition.
 - (B) Intensity of the line (cm molecule⁻¹ at 296K).
 - (C) Lorentzian collision halfwidth (cm⁻¹ atm⁻¹ at 296K).
 - (D) Energy of the lower transition level (cm⁻¹).
 - (E) Transition quantum identifications for the lower and upper levels of the transition, as the following:
 - TRS1 upper state vibrational identification,
 - TRS2 lower state vibrational identification,
 - RN1 upper state rotational identification,
 - RN2 lower state rotational identification.
- (5) The K-Q fields correspond to information related to the actual transition, in a purpose of possible intercomparison with the HITRAN database. These fields, not of prime importance for the GEISA software, contain the following parameters:
 - (F) Temperature dependence coefficient α of the halfwidth. Its value is set to zero if α is not available.
 - (G) Identification code for isotope.
 - (H) Identification code for molecule.
 - (J) Internal GEISA code for data identification.
 - (K) These fields, not of prime importance for the GEISA software, contain the following parameters:
 - (K) Molecule number.
 - (L) Isotope number (1=most abundant, 2=second, etc.).
 - (M) Transition probability (debye).
 - (N) Self-broadened halfwidth (HWHM) (cm⁻¹ atm⁻¹ at 296K).
 - (O) Air-broadened pressure shift of line transition (cm⁻¹ atm⁻¹).
 - (P) Accuracy indices for frequency, intensity and halfwidth.
 - (Q) Indices for lookup of references for frequency, intensity and halfwidth.

Table 4

Summary of the molecular species cataloged in the line parameter portion of GEISA-97 and HITRAN-96

Mol.	Mol ID		# of bands		# of isot		# Lines		F-Min (cm ⁻¹)	F-Max (cm ⁻¹)
	G	H	G	H	G	H	G	H		
H ₂ O	1	1	139	137	5	4	50217	49444	0.401	22656.465
CO ₂	2	2	626	589	9	8	62816	60802	442.006	9648.007
O ₃	3	3	108	106	5	5	281607	275133	0.026	4060.783
<u>N₂O</u>	4	4	163	162	5	5	26771	26174	0.838	5131.249
CO	5	5	104	47	6	6	13515	4477	3.414	8464.883
CH ₄	6	6	55	42	2	3	66883	40958	0.010	6184.492
O ₂	7	7	18	18	3	3	6292	6292	0.000	15927.806
NO	8	8	293	50	3	3	94738	15331	0.000	9273.214
SO ₂	9	9	9	9	2	2	38853	38853	0.017	4092.948
<u>NO₂</u>	10	10	11	11	1	1	100680	100680	0.498	2938.381
<u>NH₃</u>	11	11	34	34	2	2	11152	11152	0.215	5294.501
PH ₃	12	28	5	2	1	1	4635	2886	17.805	2445.553
<u>HNO₃</u>	13	12	12	13	1	1	171504	165426	0.035	1769.982
OH	14	13	221	103	3	3	41786	8676	0.005	19267.869
HF	15	14	6	6	1	1	107	107	41.111	11535.570
HCl	16	15	17	17	2	2	533	533	20.240	13457.841
HBr	17	16	16	16	2	2	576	576	16.232	9758.564
HI	18	17	9	9	1	1	237	237	12.509	8487.305
<u>ClO</u>	19	18	12	12	2	2	7230	7230	0.028	1207.639
<u>OCS</u>	20	19	151	7	6	4	24922	858	0.381	4118.004
H ₂ CO	21	20	10	10	3	3	2702	2702	0.000	2998.5274
<u>C₂H₆</u>	22	27	3	2	2	1	14981	4749	725.603	3000.486
<u>CH₃D</u> (§)	23	24	9	(*)	1	(*)	11524	7074	7.760	3146.460
<u>C₂H₂</u>	24	26	10	10	2	2	1668	1668	604.774	3358.285
<u>C₂H₄</u>	25	(*)	11	(*)	2	(*)	12978	(*)	701.203	3242.172
GeH ₄	26	(*)	1	(*)	1	(*)	824	(*)	1937.371	2224.570
HCN	27	23	41	8	3	2	2575	772	2.870	18407.973
C ₃ H ₈	28	(*)	1	(*)	1	(*)	9019	(*)	700.015	799.930
C ₂ N ₂	29	(*)	29	(*)	1	(*)	2577	(*)	203.955	2181.690
C ₄ H ₂	30	(*)	30	(*)	1	(*)	1405	(*)	190.588	654.425
HC ₃ N	31	(*)	31	(*)	1	(*)	2027	(*)	474.293	690.860
HOCl	32	21	6	6	2	2	15565	15565	0.024	3799.682
N ₂	33	22	1	1	1	1	117	120	2001.711	2619.230
CH ₃ Cl	34	24	8	8	2	2	9355	9355	679.050	3172.927
<u>H₂O₂</u>	35	25	2	2	1	1	100781	5444	0.043	1499.487
<u>H₂S</u>	36	31	30	11	3	3	20788	7151	2.985	4256.547
HCOOH	37	32	7	7	1	1	3388	3388	1060.962	1161.251
COF ₂	38	29	7	7	1	1	54866	54866	725.005	1981.273
SF ₆	39	30	1	1	1	1	11520	11520	940.425	952.238
C ₃ H ₄	40	(*)	1	(*)	1	(*)	3390	(*)	290.274	359.995
HO ₂	41	33	4	4	1	1	26963	26963	0.055	3675.819
ClONO ₂	42	35	3	3	2	2	32199	32199	763.641	797.741
Total			2255	1470	96	82	1346266	999361		

Underlined molecules are new or updated for GEISA-97. (§) Individual molecule in GEISA ; isotope of CH₄ in HITRAN
 (*) Molecule not included in HITRAN

isotopic species, an update of the $\{2\nu_1, \nu_1 + \nu_3, 2\nu_3\}$ cold band at 5 μm . There have also been various new inclusions or updates for several hot bands in various spectral ranges in the 10 μm to 2.5 μm region.

Table 5
Summary of differences between GEISA-97 and HITRAN-96 for molecules in common

Species	Region	v	I	γ	References
H ₂ O	2v ₂ -v ₂ lines of H ¹⁶ OD and v ₂ band of isotope 182 in the region 8.9 - 5.7 μ m, included in GEISA.	*	*	*	GEISA-92 ^{4,5} ATMOS-85 line list ¹³
CO ₂	Lines of ¹⁸ O ¹³ C ¹⁸ O, in the 4.3 μ m region, included in GEISA as well as weak intensity lines of the other isotopes.	*	*	*	GEISA-86 ¹⁴
<u>O₃</u>	The 2 regions, 5.6 - 4.3 μ m (bands 2v ₁ , v ₁ +v ₃ , 2v ₃) and 4.3 - 3.6 μ m [bands v ₁ +2v ₂ , 2v ₂ +v ₃ , 3v ₃ -v ₂ , and (v ₁ +2v ₂ +v ₃)-v ₂] updated for GEISA.	*	*	*	Refs. 15-34
<u>N₂O</u>	The entire 19 - 16 μ m region has been reworked. This includes 11 bands (band v ₂ +v ₃ -v ₃ new band).	*	*	*	Refs. 35-41
CO	Transitions with v'' \leq 8 present in GEISA (v'' \leq 1 in HITRAN).	*	*	*	GEISA-92 ^{4,5}
<u>CH₄</u>	New predictions in the regions 11 - 5 μ m and 5.2 - 2.8 μ m.	*	*	*	TDS ^{9,10} Refs. 42-49
<u>NO</u>	New spectroscopic line parameters for ¹⁴ N ¹⁶ O in the region from microwaves to 1.07 μ m.	*	*	*	Refs. 50-62
PH ₃	Whole GEISA content in the region 561.6 - 4.1 μ m different from HITRAN content.	*	*	*	GEISA-86 ¹⁴ GEISA-92 ^{4,5}
<u>HNO₃</u>	3v ₉ -v ₉ and v ₅ +v ₉ -v ₉ bands present in HITRAN replaced by new data for band v ₅ +v ₉ -v ₉ in the region 12.6 - 10.5 μ m.	*	*	*	Refs. 87-95
<u>OH</u>	New data for the whole content of ¹⁶ OH in the region from the microwaves to 2.4 μ m.	*	*	*	Refs. 96-106
<u>OCS</u>	Region 20.4 - 2.4 μ m entirely updated in GEISA. Two new isotopes, ¹⁶ O ¹² C ³³ S and ¹⁶ O ¹³ C ³⁴ S implemented.	*	*	*	Refs. 116-141
<u>C₂H₆</u>	Band v ₉ in the region 13 - 11 μ m. Band v ₁₂ new isotope ¹² C ¹³ CH ₆ in the region 13.7 - 10.9 μ m.	*	*	*	GEISA-92 ^{4,5} Refs. 142-147
<u>CH₃D</u>	New list for the triad v ₃ , v ₅ , v ₆ in the region 11.8 - 5.7 μ m (Independent molecule in GEISA; isotope of CH ₄ in HITRAN).	*	*	*	Refs. 148-149
HCN	The whole content in the 1.7 - 0.5 μ m region.	*	*	*	GEISA-92 ^{4,5}
N ₂	The whole content in the 5 - 3.8 μ m region.	*	*	*	GEISA-92 ^{4,5}
H ₂ O ₂	The whole content with new predictions in the region from the microwave to 6.7 μ m	*	*	*	Patrín et al. Ref. 169
H ₂ S	New predictions in the 4 μ m and 2.7 μ m regions				Brown et al. Ref. 171

Underlined molecules have been updated for GEISA-97 edition. * existing difference

For the ¹⁶O¹⁷O¹⁶O and ¹⁷O¹⁶O¹⁶O isotopic species of ozone, the v₂ band at 17 μ m was included for the first time in the GEISA database using linelists generated in 1991 by Rinsland et al. [15]. The parameters used for the line position calculations (i.e. the rotational parameters in both the upper and lower vibrational state and the band centers) were deduced by combining the results

from the analysis of Fourier transform infrared measurements at 17 μm to existing microwave measurements [15]. For the intensities, the dipole moments were deduced from theoretical considerations [16] for the $^{16}\text{O}^{17}\text{O}^{16}\text{O}$ symmetric isotopic species and from a calibration of the $^{16}\text{O}^{17}\text{O}^{16}\text{O}/^{17}\text{O}^{16}\text{O}^{16}\text{O}$ relative intensities for the non symmetric $^{17}\text{O}^{16}\text{O}^{16}\text{O}$ isotopic species.

For the main $^{16}\text{O}_3$ isotopic species, numerous high-resolution laboratory studies or theoretical studies [17–27] were performed in the far-infrared to mid-infrared region in order to determine assignments, positions and intensities for many weaker bands of ozone or to extend the accuracy of the already existing line positions and intensities. These efforts lead to an extension of the ozone database which was generated in 1990 by Flaud et al. [16] Added to these works, and in the frame of the preparation of the IASI mission, the following updates have been made for GEISA-97.

The 5.6–3.6 μm spectral region: This spectral region corresponds to the triad $2\nu_1$, $\nu_1 + \nu_3$, $2\nu_3$. The improvement of the FTS signal/ratio and the special experimental setup (36 m \times 40 Torr) have allowed transitions to be observed down to 4×10^{-26} cm molecule $^{-1}$ at 296 K. For this region, the residual r.m.s. is 0.11×10^{-3} cm $^{-1}$ for 2421 fitted line positions, and the residual r.m.s. for the intensities is 2.4% [23].

The 4.3–3.6 μm spectral region: The cold bands $\nu_1 + 2\nu_2$ and $2\nu_2 + \nu_3$ have been observed up to J and K_a equal to 55 and 11, respectively [24]. The final fit on 615 energy levels is 0.39×10^{-3} cm $^{-1}$ and $\pm 8.8\%$ for the intensities [24]. In addition, the two hot bands, $\nu_1 + 3\nu_2 - \nu_2$ and $3\nu_2 + \nu_3 - \nu_2$, have been obtained by Barbe et al. [25]. The precisions for the weak bands are obviously coarse: 1.9×10^{-3} cm $^{-1}$ for the positions and $\pm 15\%$ for the intensities. The $3\nu_3 - \nu_2$ and $\nu_1 + 2\nu_3 - \nu_2$ bands have been observed [24] with accuracies similar to those of other hot bands mentioned above.

The 5.6–6.2 μm spectral region: In this spectral region, where the $3\nu_2 - \nu_2$ and $2\nu_3 - \nu_2$ bands were never identified before, the bands $2\nu_2$, $3\nu_2 - \nu_2$, $\nu_1 + \nu_3 - \nu_2$ and $2\nu_3 - \nu_2$ have been located and analyzed. The new results will be available for the next database edition. The range of assigned wavenumbers is also larger than in previous studies as it goes up to $J = 57$ and $K_a = 16$ for the $2\nu_2$ line positions. Absolute accuracy of the intensities is 11%.

The 3.6 μm spectral region: Starting from the analysis of $\nu_1 + 2\nu_2 + \nu_3$, appearing at 2.9 μm [26], the hot band $(\nu_1 + 2\nu_2 + \nu_3) - \nu_2$ has been calculated efficiently, newly confirmed by laboratory measurements [27] and included in the database.

The value of the n coefficient (temperature dependence of the air broadened halfwidth coefficient) obtained by Barbe et al. [28] $n = 0.72 \pm 0.08$ has been adopted for all the transitions in the infrared. It should be noticed that the value of $n = 0.76$ was previously obtained by Gamache et al. [29] in 1985.

Air- and self-broadened halfwidths (γ_{air} and γ_{self} , respectively) are from a mixture of experimental and theoretical values. Most of the data are from a database of N_2 -broadened theoretical values [30] which covers the range of $J'' \leq 35$. The algorithm to add the halfwidths to the O_3 transitions operates as follows: given an initial and final state the theoretical database is searched for data. If available the N_2 -broadened value is used. When there is no value in this database and $J'' < 40$, an averaged theoretical halfwidth is used. For both of these cases, the value is then scaled by 0.95 to get the corresponding air-broadened value [31] and increased by an additional 9%, as recommended by Smith [32]. For air broadening, for transitions with $J \geq 40$, the polynomial expression of Rinsland [33] is used. For the halfwidths, the polynomial expression of Smith et al. [34] which was determined by a fit to 355 measurements, is used.

Table 6
New or updated linelist for $^{16}\text{O}_3$ in GEISA-97

Spectral Range (μm)	Vibrational Transition
10	{(003),(102),(201),(300)}-{(200),(101),(002)}
4.8	{(003),(102),(201),(300)}-{(100),(001)} {(002),(101),(200)}- (000)
4.4	{(021),(120)}- (000) (003) - (010) (102) - (010)
3.6	(121) - (010)
3.3	{(003),(102),(201),(300)}- (000) {(004),(103),(310)}-{(100),(001)} {(013),(112)}- (010)
3.0	{(004),(103),(310)}- (010)
2.7	{(013),(112)}- (000)
2.5	{(004),(103),(310)}- (000)

The summary of the new, improved or updated $^{16}\text{O}_3$ transitions included in GEISA-97 is given in Table 6.

3.2. N_2O (molecule 4)

New high-resolution FTIR intensity measurements of the $17\ \mu\text{m}$ ν_2 fundamental and associated hot bands have been reported by Johns et al. [35] and Weber et al. [36]. The linear Herman–Wallis factor for the ν_2 band and hot bands, which has been determined for the first time, is unusually large and, consequently, the R-branch is much stronger than the P-branch. Neglecting the Herman–Wallis effect can lead to an error in the line intensities of about 30% at $J = 30$, as explained in Ref. [35]. The accuracy of the line intensities for the four bands, ν_2^e , $2\nu_2^{2e} \leftarrow \nu_2^{1e}$, $2\nu_2^{2f} \leftarrow \nu_2^{1f}$, and $2\nu_2^{0e} \leftarrow \nu_2^{1e}$ in the ν_2 bending modes are in the order of $\pm 5\%$ and better [35, 36].

The entire bending mode region has been updated including all bands from the compilation by Maki and Wells [37], which comprises 10 bands of the major isotopomer and the three fundamentals of the 14-15-16, 15-14-16, and 14-14-18 isotopomers. Transition frequencies and intensities are taken from Ref. [37], except for the line intensities of the bands reported by Johns et al. [35] and Weber et al. [36]. Temperature dependent broadening coefficients for N_2 - and self-broadening have been determined by Weber et al. [36], who included broadening data from other vibrational bands [38–41] to obtain a good temperature coverage. The accuracy of the widths are conservatively estimated to be about 5% and better.

3.3. CH_4 (molecule 6)

The changes made for GEISA-97 have been the replacement of several sets of data on the main isotope $^{12}\text{CH}_4$ and the introduction of new data on $^{12}\text{CH}_4$ and $^{13}\text{CH}_4$. These are essentially based

on the information which was previously available only at the specialized database for spherical top molecules: TDS/STDS [9, 10].

The 900–2000 cm⁻¹ spectral region: A new prediction containing over 6000 transitions of the v_2/v_4 dyad of ¹²CH₄ with an intensity threshold of 10⁻²⁶ cm molecule⁻¹ at room temperature was included. These data refer to previously reported works [42, 43]. A new prediction of the pentad-dyad hot band system containing over 18,800 transitions with the same threshold was incorporated representing a sensible improvement with respect to previously existing data, owing to recent works [44, 45].

The 2000–3500 cm⁻¹ spectral region: Three sets of data were included in replacement of previously existing data. The first two sets consist of 13,397 (resp. 4240) transitions of the $v_1/v_3/2v_2/v_2 + v_4/2v_4$ pentad of ¹²CH₄ (resp. ¹³CH₄) with an intensity threshold of 10⁻²⁵ cm molecule⁻¹ at room temperature referring to previously reported works [44] (resp. Ref. [46]). The third set is a new prediction of the octad-dyad hot band system containing 13,363 transitions with the same threshold referring to preliminary results of work in progress [47].

For consistency with current studies on excited states and with the specialized TDS databank [9] and STDS package [10] for spherical top molecules, a new nomenclature of the energy levels for the ¹²CH₄ and ¹³CH₄ species has been adopted. As a matter of fact, different specific quantum numbers and nomenclatures were used in earlier predictions, derived from partial analyses of some isolated excited states of ¹²CH₄. These notations are no longer adapted to more efficient polyad treatments. Thus, the labelling of all the energy levels of methane was chosen to refer only to quantum numbers relevant to all vibrational states. Approximate quantum numbers valid only in few specific cases were eliminated. This approach is especially aimed at providing the non expert database user with reliable information in a form adapted for both fundamental and excited states (including those expected from future work). Precisely, each vibration-rotation energy level is labelled by the set of numbers:

$$v_1 v_2 v_3 v_4 \text{ percent } J C n$$

where the v'_s are the principal vibrational quantum numbers of the normal mode basis function upon which the eigenfunction has the largest projection, quoted by “percent”. J is the usual rotational quantum number, C the conventional rovibrational symmetry in the Td group, and n an integer numbering the eigenvalues in increasing order within the polyad scheme.

An estimate of the self-broadened linewidths has been included in the new ¹²CH₄ and ¹³CH₄ files, according to the empirical mean values proposed in Ref. [48].

The permanently updated source of the modeled positions and intensities on ¹²CH₄ and ¹³CH₄ (as well as on other spherical top molecules) is freely accessible from the STDS package [10] by ftp on the web site at <http://www.u-bourgogne.fr/LPUB/sTDS.html>. The TDS information system [9, 49] is designed for an advanced modelling of various spectroscopic processes for methane, including absorption/transmission, Raman, Stark, two-photon, under extended conditions using these data.

3.4. NO (molecule 8)

In GEISA-97 the 46 species of NO (¹⁴N¹⁶O) has been updated, from the far infrared to 9273 cm⁻¹, by extensive recent and new results of spectral parameters from the University of

Denver (DU) database, providing significant improvements since GEISA-92. An extensive use of the recent advances in NO has been described by Goldman [50, 51] for generating new line parameters with high v and J , for both pure rotation and vibration–rotation transitions in $X^2\Pi$. This update is a direct extension of the work on updating the $X^2\Pi$ lines of OH by Goldman et al. [52]. The new set for NO is composed of the $\Delta v = 0, \dots, 5$ dipole allowed transitions between $v = 0, \dots, 14$ and J up to 125.5, with low-intensity cutoffs, applicable to both atmospheric and high-temperature research. In all, line parameters for 75 separate bands were calculated: 15 pure rotation bands and 60 vibration–rotation bands. In this work, the Hamiltonian constants of Coudert et al. [53] for A -doubling were used for the rovibrational states of $v = 0, 1, 2$ and for all the line transitions between these states.

The line intensity calculations are based on an improved calculational method for the vibrational–rotational wavefunctions [54] and a combination of the experimental and theoretical electric dipole moment functions [55]. The derived intensities are significantly improved compared to those available for use in GEISA-92.

The recent halfwidths study by Spencer et al. [56] has extended the previous works of Falcone et al. [57], Houdeau et al. [58], Phillips and Walker [59], Ballard et al. [60] and Spencer et al. [61] and provided (0–1) band $^2\Pi_{1/2}, ^2\Pi_{3/2}$ NO–N₂ halfwidths with temperature-dependent coefficients.

In the work of Goldman [50] and Goldman et al. [51], the results of Ref. [56] have been adopted for J up to 16.5 for all bands, and single values for higher J 's have been assumed. The correction to NO–Air halfwidths was determined assuming $\gamma_{\text{NO–Air}}^0 = 0.79\gamma_{\text{NO–O}_2}^0 + 0.21\gamma_{\text{NO–O}_2}^0$, with $\gamma_{\text{NO–O}_2}^0 = 0.05$, based on Ref. [58]. The self-broadening (0–2) $^2\Pi_{1/2}, ^2X_{3/2}$ halfwidths of Pine et al. [62] have been adopted, as they may be more consistent with the results of Spencer et al. [56] than with Ballard et al. [60]. Compiling a set for the “best” halfwidths values still requires an additional study. It should also be noted that the pressure shift coefficients provided by Pine et al. [62] and Spencer et al. [61] have not been incorporated into the NO new data issued from the University of Denver database. Accuracy codes for the line positions, intensities, and halfwidths have not been estimated yet. It is clear, however, that lines of $v' = 0, 1, 2$ and $J' < 50$ have high position accuracy, of 0.0001–0.001 cm⁻¹, and intensity absolute accuracy of 5–15%.

Significant post-GEISA-97 and HITRAN-96 work has been done, and described in Ref. [51]. The corresponding results will be included in the next edition of the GEISA database.

3.5. SO₂ (molecule 9)

SO₂ is well known to be of astrophysical importance. Also, SO₂ plays a large role in the chemistry of planetary atmospheres. In the Earth's atmosphere, SO₂ may be produced both by man made or by volcanic eruptions, and is responsible for the production of acid rain. Once in the stratosphere, sulfur dioxide is converted into sulfate aerosols which affect both stratospheric chemistry and climate as explained in Goldman et al. [63] and Mankin et al. [64].

The GEISA database provides SO₂ parameters in seven different spectral regions, namely the microwave and far infrared spectral region which corresponds to transitions within the ground vibrational state, and the 19.3, 8.6, 7.3, 4, 3.7 and 2.5 μm spectral regions which correspond to the ν_2 band, the ν_1 band, the ν_3 band, the $\nu_1 + \nu_3$ and $\nu_1 + \nu_2 + \nu_3 - \nu_2$ bands, the $2\nu_3$ band and the $3\nu_3$ band, respectively. The corresponding linelists were extensively described in Ref. [4]. Here are only given comments concerning the spectral ranges recently updated and included in GEISA-97.

The 4 μm spectral region: This spectral region corresponds to the $\nu_1 + \nu_3$ band and to the $\nu_1 + \nu_2 + \nu_3 - \nu_2$ associated first hot band. Although about 60 times weaker than the ν_3 band, which is the strongest infrared band of SO₂, the $\nu_1 + \nu_3$ band corresponds to a rather clear atmospheric window and is then of atmospheric importance. This spectral range was recently updated for the ³²S¹⁶O₂ isotopic species. Compared to the previous linelists quoted in GEISA-92 [4] for the $\nu_1 + \nu_3$ and $\nu_1 + \nu_2 + \nu_3 - \nu_2$ bands, these new linelists correspond to significant improvements in accuracy both for line positions and line intensities [65]. Actually, the line positions were generated using new experimental data recorded by difference frequency laser spectrometer, and for the line position calculations, the vibrational–rotational resonances were explicitly taken into account for the first time.

On the other hand, the line intensities were derived using both high- and medium-resolution experimental data, leading to values of the total band intensity 0.539×10^{-18} and 0.423×10^{-19} cm molecule⁻¹ for the $\nu_1 + \nu_3$ and $\nu_1 + \nu_2 + \nu_3 - \nu_2$ bands, respectively. These values differ significantly from the previous ones quoted in GEISA-92 (0.395×10^{-18} and 0.211×10^{-19} cm molecule⁻¹). It is worth noticing that the ³⁴S¹⁶O₂ isotopic variant of the $\nu_1 + \nu_3$ band has not been updated in GEISA-97, and that the ratio of the ³⁴S¹⁶O₂ and ³²S¹⁶O₂ band intensity for the $\nu_1 + \nu_3$ band ($0.603 \times 10^{-20}/0.539 \times 10^{-18}$) differs significantly from the isotopic ratio of these two isotopic species i.e. the isotopic ratio ³⁴S¹⁶O₂/³²S¹⁶O₂ = 0.044. Consequently, for the ³⁴S¹⁶O₂ isotopic variant the $\nu_1 + \nu_3$ band may need improvement in the future version of GEISA.

The 3.7 μm spectral region: This spectral range corresponds to the $2\nu_3$ band of ³²S¹⁶O₂. The corresponding line parameters have been introduced for the first time in GEISA-97 using the $2\nu_3$ line positions and line intensities obtained recently by Lafferty et al. [66]. These parameters were derived from the analysis of spectra recorded by difference-frequency laser spectroscopy. For the line position and line intensity calculations the rovibrational resonances involving the (002) and (130) energy levels were explicitly taken into account.

The 2.5 μm spectral region: This spectral range corresponds to the $3\nu_3$ band of SO₂: the linelist related with this rather weak band of ³²S¹⁶O₂ was introduced in the GEISA database because this spectral region corresponds to an infrared window for the Venus atmosphere, and because the Q branch structure of the $3\nu_3$ band at 4050 cm⁻¹ was clearly identified in the Venus infrared spectrum [67]. These $3\nu_3$ line parameters were generated from extensive line position and line intensity studies [68, 69] performed using various techniques (Fourier transform spectra and difference-frequency laser measurements) and taking into account all the relevant rovibrational resonances.

3.6. NO₂ (molecule 10)

Because of its importance in the photochemistry of the stratosphere this molecule has been the subject of numerous studies. In the GEISA database, four spectral domains involve ¹⁴N¹⁶O₂, namely, the pure rotation region, and the 13.3, 6.2 and 3.4 μm regions.

For ¹⁴N¹⁶O₂ it is necessary to take into account the doublet structure due to the electron spin–rotation interaction together with, depending on the spectral range, the hyperfine structure due to interactions involving the nitrogen nuclear spin ($I = 1$). Also, starting from the first triad of interacting states, the rovibrational interactions must be considered in the calculations. The line parameters presently available in GEISA for NO₂ are extensively described in Refs. [4, 70]

Consequently, only the 13.3 and 6.2 μm spectral ranges, which were recently updated for GEISA-97, will be described here.

The 13.3 μm region: A new linelist has been generated for the ν_2 band, taking into account the hyperfine interaction together with the spin–rotation interaction. Actually, this update was performed in GEISA-97 because a new analysis of this band, by Perrin et al. [71] has shown that the hyperfine structure is easily observable in some parts of the ν_2 band. Also, the first hot band $2\nu_2 - \nu_2$ (i.e. the (020)-(010) vibrational transition), which was not present in the previous versions of the database, was included in this linelist: for this hot band, the hyperfine structure was not modelled. For these two linalists generated in the 13 μm region, experimental line positions obtained from Fourier transform spectra [71] have been used as well as ν_2 experimental lines intensities measured by Malathy Devi et al. [72].

The 6.2 μm region: The 6.2 μm region corresponds to the strongest infrared band of this molecule which is then commonly used for measurements of atmospheric nitrogen dioxide from borne experiments (balloon or satellite). Because of the importance of the 6.2 μm region, the spectral linalists corresponding to the ν_3 band (which is the main cold band in this region), and to the ν_1 and $2\nu_2$ interacting cold bands, were updated in GEISA-97. This new linelist was generated, using, for the line position calculations, a theoretical model which takes explicitly into account the $(100) \Leftrightarrow (001)$ and the $(020) \Leftrightarrow (001)$ first and second order Coriolis interactions affecting the rovibrational levels. Furthermore, the contribution to the energy levels due to the spin–rotation interaction was taken into account explicitly in this new linelist. It has to be recalled that this interaction was only taken into account through a perturbation method in the previous GEISA-92 version [4]. The parameters used to generate the new linelist [73] have been obtained through new FTS measurements performed on line positions [73] and line intensities [74, 75] for the ν_1 , $2\nu_2$ and ν_3 interacting cold bands.

3.7. NH_3 (molecule 11)

The GEISA-97 line parameters are similar to the HITRAN-96 [8] ones and are used without further revision. In this, there were three major changes. Ammonia parameters appeared for the 2100 to 5300 cm^{-1} region for the first time. Air- and self-broadened line widths were obtained from a polynomial fit of laboratory measurements. The notation of the rotational quantum numbers was also standardized for the transitions of the main isotope. The new parameters above 2100 cm^{-1} were based on four new studies [76–79] of the band systems at 4, 3, 2.3 and 2 μm . In the 4 μm study by Kleiner et al. [76] transitions and intensities of $3\nu_2$ and $\nu_2 + \nu_4$ were modeled to $\pm 0.007 \text{ cm}^{-1}$ for positions and $\pm 6\%$ for intensities. Empirical measurements of some 270 unassigned lines were also included with lower state energies set to 300 cm^{-1} . At 3 and 2.3 μm , predictions provided by S. Urban were made based on the energy level analyses of Guelachvili et al. [77] and Urban et al. [78], respectively. The uncertainties of the positions vary greatly for these two regions from 0.001 to 0.3 cm^{-1} . The intensities in the ν_1/ν_3 region should also be reconsidered in future updates. For example, for the ν_1 and ν_3 fundamental, the database uses band intensities [80] of 20.5 and 21.4 $\text{cm}^{-2} \text{ atm}^{-1}$ while Pine and Dang-Nhu [81] reported values of 22.3 and 13.1 $\text{cm}^{-2} \text{ atm}^{-1}$. Similarly, the database choice for the band strengths of $\nu_1 + \nu_2$ and $\nu_2 + \nu_3$ are 2.8 and 16.1 $\text{cm}^{-2} \text{ atm}^{-1}$ compared to the Margolis and Kwan [82] values of 2.71 and 19.0 $\text{cm}^{-2} \text{ atm}^{-1}$. A new study of the 3 μm region, in progress by Kleiner et al. [83] will correct some of the problems

with the current prediction. At 2 μm , the empirical linelist of Brown and Margolis [79] was incorporated, including lower state energies from confirmed assignments, from empirically determined estimates obtained from measuring intensities at different temperatures. The uncertainties for the positions and intensities are thought to be 0.0005 cm^{-1} and $\pm 6\%$, respectively.

The line widths in the database are based on the measurements of Pine et al. [84] and Markov et al. [85] using the simple polynomial expression determined by Brown and Plymate [86], in the case of NH_3 broadened by H_2 . These expressions were applied to all ammonia transitions for $J' < 13$, and default values of 0.06 and $0.4\text{ cm}^{-1}\text{ atm}^{-1}$ were used for air- and self-broadening widths at higher J . The uncertainties of the widths are thought to range from 10 to 25%.

3.8 HNO_3 (molecule 13)

Nitric acid is well known to be an important reservoir in (NO_x) and (HO_x) chemical species in the normal stratosphere. In the GEISA database, nine spectral regions involve the HNO_3 molecule; namely, the microwave region, the 22 μm (ν_9 band), 17 μm (ν_7 band), the 15.5 μm (ν_6 band), the 13 μm (ν_8 band), the 11 μm (ν_5 , $2\nu_9$, $\nu_5 + \nu_9 - \nu_9$ bands), the 8.3 μm ($\nu_8 + \nu_9$ band), the 7.5 μm (ν_3 and ν_4 bands) and the 5.9 μm (ν_2 band) spectral regions. The present status of HNO_3 line parameters has been recently reviewed in detail by Goldman et al. [87]. The two strongest infrared bands of HNO_3 are in the 5.9 and 7.5 μm regions, but the HNO_3 retrievals are somehow inhibited in these spectral regions because of the existence of interfering lines from ozone and water. On the other hand, the region at 11 μm which corresponds to weaker bands is centered at an atmospheric window and has been used extensively for derivation of the vertical profile of HNO_3 and may be used for the ground-based measurements. This 11 μm region has been updated for the 1997 edition of GEISA. Two sets of line parameters were generated for the $\{\nu_5, 2\nu_9\}$ interacting cold bands and for the $\nu_5 + \nu_9 - \nu_9$ hot band.

The $\{\nu_5, 2\nu_9\}$ interacting bands: Using new Fourier transform spectra, a new extensive analysis of the $\{\nu_5, 2\nu_9\}$ interacting bands was performed, leading to very accurate line positions and relative line intensities for these two bands [88, 89]. According to the recommendations of Goldman et al. [87, 90] the line intensities were calibrated to the absolute line intensities measured by Giver et al. [91].

When dealing with the line positions, an Hamiltonian model which accounts both for the Fermi- and Coriolis-type resonances was used, and a new and more accurate line list was generated.

The most significant improvements, as compared to GEISA-92, involve mainly the spectral regions corresponding to the wings of the P- and R- branches and to the ν_5 and $2\nu_9$ Q branches.

The $\nu_5 + \nu_9 - \nu_9$ hot band: The parameters which were quoted previously for the $3\nu_9 - \nu_9$ hot bands in GEISA-92 were removed from the present version of the database because a more recent study by Perrin et al. [92] demonstrated clearly that these parameters are not correct. The $\nu_5 + \nu_9 - \nu_9$ hot band gives rise to a strong and very narrow Q branch at 885.42 cm^{-1} which is easily observable in stratospheric spectra as explained in Ref. [87]. Preliminary line parameters have been generated [93] leading to a reasonably accurate linelist of this $\nu_5 + \nu_9 - \nu_9$ hot band which was then updated in GEISA-97.

The air-broadened halfwidths and the temperature-dependent coefficient [94] were retained from GEISA-92. Air-broadened widths of $0.11\text{ cm}^{-1}\text{ atm}^{-1}$ at $T = 296\text{ K}$ and the temperature-dependence coefficient of $n = 0.75$ have been taken from May and Webster [95]. No

self-broadened halfwidths value is included; however, it was listed as $0.73 \text{ cm}^{-1} \text{ atm}^{-1}$ at $T = 296 \text{ K}$ [94].

3.9. OH (molecule 14)

The GEISA-92 data for the main isotope 61 (^{16}OH) have been removed to be replaced by the results issued from a significant update of the OH $X^2\Pi-X^2\Pi$ line parameters recently completed by Goldman et al. [52]. The new set is composed of the $\Delta v = 0, \dots, 6$ dipole-allowed transitions between $v = 0$ and $v = 10$, with J up to a maximum value of 49.5, with low-intensity cutoffs applicable to both atmospheric and high-temperature studies. In all, line parameters for 56 separate bands were calculated: 11 pure rotation bands and 45 vibration–rotation bands with both main and satellite branches. The transition frequencies were determined from three different sets [96–98] of calculated term values in order to have the most accurate set of line positions over a wide range of both vibration and rotation quantum numbers.

More accurate line intensities have been reported owing to improved transition moment integrals. This was achieved by using an improved method [99] for calculating vibrational wavefunctions for the $X^2\Pi$ states of OH, in conjunction with the latest OH dipole moment function [100].

In addition to updating the line parameters themselves, estimates accuracy indices [101] have been included for the uncertainties associated with the line parameters.

The single value, $0.083 \text{ cm}^{-1} \text{ atm}^{-1}$, for the air-broadened halfwidth assigned to all OH lines in GEISA-92 dates back to 1979 [102]. This corresponds to the measured halfwidths of the transitions around 13.4 GHz between the four levels with $v = 0$ and $J = 7/2$. A number of recent papers [103, 104] (who also presented evidence for collisional narrowing) [105] extend the range of J values whose halfwidths are measured, and also cast doubts about the accuracy of the former results [102]. Considering these newly measured halfwidth values, and achieving proper theoretical processing, we have adopted $T = 296 \text{ K}$ halfwidths of 0.095, 0.086, 0.065 and $0.053 \text{ cm}^{-1} \text{ atm}^{-1}$ for $N = 1, \dots, 4$, respectively, and $0.040 \text{ cm}^{-1} \text{ atm}^{-1}$ for $N > 4$ (as described in Ref. [52]).

The temperature dependence of the halfwidths has been evaluated using a theoretical study by Buffa et al. [106]. The values vary between 0.59 and 0.72, from which the average value of 0.66 was adopted for all lines.

Complete details on the procedures used for the new data set are given in Ref. [52]. Due to a lack of available experimental data neither values were assigned for the air-broadened pressure shift, nor for the self-broadened halfwidth.

3.10. ClO (molecule 19)

In GEISA-97, improved line parameters for the $X^2\Pi-X^2\Pi$ (1–0) bands of ^{35}ClO and ^{37}ClO have replaced the former existing ones in GEISA-92, with more accurate line positions and intensities. The new parameters were calculated as described by Goldman et al. [107] on the basis of the work of Burkholder et al. [108, 109].

The absolute accuracy of the line positions is estimated as $\pm 0.0003 \text{ cm}^{-1}$. After normalization to the laboratory value of $S = 9.68 \pm 1.45 \text{ cm}^{-2} \text{ atm}^{-1}$ at 296 K [109], the integrated band

intensity corresponds to 3.904×10^{-19} cm molecule⁻¹ at 296 K, compared to 4.884×10^{-19} cm molecule⁻¹ at 296 K adopted for GEISA-92.

The value $\gamma^0 = 0.093 \pm 0.018$ cm⁻¹ atm⁻¹ at 296 K has been adopted for the air collisional broadening coefficient for all lines. It is the same as that for the N₂ broadening obtained in Ref. [109]. Following the results obtained by Rinsland and Goldman [110], the value of 0.75 was used for the *n* coefficient (temperature dependence of the air broadened halfwidth coefficient).

New experimental line intensities have been recently obtained by Birk and Wagner [111] providing a corresponding measured band intensity of 9.01 ± 0.27 cm⁻² atm⁻¹ at 296 K, and thus smaller by up to $\sim 7\%$ from the GEISA-97 value. Note that individual lines, however, are smaller by up to $\sim 10\%$ in intensity. These will be incorporated into the future Edition of GEISA.

The pure rotation ClO lines have been kept from GEISA-92, originating from the JPL catalog of 1985 [112]. The latest JPL catalog [113], however, contains both $v = 0$ and $v = 1$ lines, while GEISA contains only $v = 0$ lines. Also, the updated parameters of the ClO lines used for Microwave Limb Sounder (MLS) on the Upper Atmosphere Research Satellite (UARS), as described by Waters et al. [114] and by Oh and Cohen [115], have not been yet incorporated into GEISA.

3.11. OCS (molecule 20)

Since GEISA-92, the region 490–4116 cm⁻¹ has been totally reviewed and two new isotopes have been added: ¹⁶O¹²C³³S and ¹⁶O¹³C³⁴S, coded respectively 623 and 634. The main IR bands of carbonyl sulfide up to 3100 cm⁻¹ and the $2\nu_3$ band near 4100 cm⁻¹ have been generated.

The frequencies correspond to calculated spectra on the basis of the global analysis developed for this molecule [116–118]. The global analyses of the main isotopomers are regularly updated using new experimental data published in the literature. From the last published global analysis [118] many quite accurate data have been introduced (see Refs. [119–131]), giving a sensitive improvement of the accuracy of the analyses. A statistical agreement is obtained with all the available data.

Many hot bands and isotopomer's bands are included. The list of codes for the isotopic species and for the vibrational states has been extended. Vibrational states are given by v_1, v_2, l_2, v_3 , where v_3 corresponds to the asymmetric stretching mode near 2060 cm⁻¹.

Intensities are based on papers of Kagann [132] for the 500, 1650 and 4000 cm⁻¹ regions, of Dang-Nhu et al. [133] for the 2575 cm⁻¹ region, of Bouanich et al. [134] for the 850 cm⁻¹ region, of Blanquet et al. [135] for the 1000 cm⁻¹ region, and of Belafhal et al. [126, 127] for the 1800–3200 cm⁻¹ region. The intensities for the 2500–3100 cm⁻¹ region [126] have been recalibrated according to more accurate measurements performed by Errera et al. [136]. Some intensities from Ref. [126] have been improved on the basis of spectra recorded by Brown [137]. The intensities of the $\nu_1 + 2\nu_2$ band near 1900 cm⁻¹ have been multiplied by a factor 1.22, those of the ν_3 band near 2000 cm⁻¹ by 0.88, and those of the $4\nu_2$ band near 2100 cm⁻¹ by 1.10. The validity of those corrections has been recently confirmed by Strugariu et al. [138] and the absolute precision of the intensity of most lines is of the order or better than 10%. Note that the intensities of the $2\nu_3$ band of ¹⁶O¹²C³²S are to be multiplied by 1.07 to agree with the more accurate values recently published by Bermejo et al. [139].

The air-broadened widths were taken from Refs. [140, 141], while the self-broadened values reported by Bouanich et al. [134] were employed. The coefficients of the temperature dependence of the self-broadened widths were assumed for the air-broadened widths. Default constant values were set at higher J (J greater than 67 for air-, 75 for self- and 60 for the temperature coefficient).

The improvements on the GEISA-97 OCS contents, since GEISA-92, are summarized in Table 7. Column 1 lists the isotopes identification codes (ISOT ID) and column 2 the number of lines (LINES) existing in the spectral interval corresponding to the upper vibrational state E' (column 3) and the lower vibrational state E'' (column 4). The upper and lower vibrational states are identified as explained above. In columns 5 and 6 are the minimum (NU.MIN) and the maximum (NU.MAX) frequencies (cm^{-1}) in the actual spectral interval. The related minimum (MIN.I) and maximum (MAX.I) intensity values are in columns 7 and 8, respectively, and the total line intensities sum (SUM.I) in column 9, in cm molecule^{-1} .

A total of 147 bands have been updated or newly introduced in GEISA-97. This corresponds to 24 547 entries (OCS whole content: 24 922 entries).

3.12. $^{13}\text{C}^{12}\text{CH}_6$ (molecule 22)

Motivated by the recent discovery of the minor isotopomer of ^{13}C -ethane in the planetary atmospheres of Jupiter [142] and Neptune [143], high-resolution laboratory measurements of the ν_{12} fundamental (which is equivalent to ν_9 of the major isotopomer) centered at 821 cm^{-1} were carried out by Kurtz et al. [144] and Weber et al. [145, 146] using a FTIR and tunable diode laser (TDL) spectrometer. The very high spectral resolution of the TDL spectrometer was utilized to facilitate the determination of the barrier to internal rotation of the two methyl groups [146]. Molecular constants for ν_{12} were derived from a global analysis, which included the treatment of a high-order torsional Coriolis interaction with the torsional $\nu_6 = 3$ state (high barrier limit).

Selected line intensities have been determined from the high-resolution FTIR measurements, and a dipole moment for the band strength was obtained [146]. In the compilation of line intensities for the entire band, intensity perturbation due to the torsional Coriolis interaction, was taken into account [146, 147]. The absolute uncertainty in the frequencies is of the order of 0.0005 cm^{-1} and that in the intensities is less than 5%.

3.13. CH_3D (molecule 23)

The data on the lowest $\nu_3/\nu_5/\nu_6$ triad of $^{12}\text{CH}_3\text{D}$ were replaced by a new prediction derived from a recent work by Nikitin et al. [148] yielding an improved accuracy of about one order of magnitude on the line positions. This work represents the first step of a global description of the infrared spectrum of this molecule using a theoretical approach in which the rovibrational effects analysed within the triad system can be extrapolated to the nonad system ($2400\text{--}3200 \text{ cm}^{-1}$) [149].

3.14. C_2H_2 (molecule 24)

In the $13.7 \mu\text{m}$ region several bands in the ν_5 bending mode of acetylene have been re-analyzed using high-resolution FTIR spectra recorded at 0.0025 cm^{-1} spectral resolution. From a global analysis, molecular constants for both bending vibrations of ν_4 and ν_5 up to the $2\nu_4$ and $3\nu_5$

Table 7
Summary of GEISA-97 OCS updates

ISOT ID	LINES	E'	E''	NU.MIN (cm ⁻¹)	NU.MAX (cm ⁻¹)	MIN.I	MAX.I (cm molec ⁻¹)	SUM.I
622	254	0110	0000	490.686	558.791	1.050D-23	3.890D-21	2.961D-19
632	124	0110	0000	491.130	526.204	1.010D-23	4.280D-23	2.861D-21
622	426	0220	0110	495.865	554.499	1.080D-23	6.170D-22	9.471D-20
622	142	1110	1000	497.395	536.598	1.030D-23	5.970D-23	4.198D-21
624	186	0110	0000	499.000	547.220	1.020D-23	1.700D-22	1.288D-20
622	216	0200	0110	501.964	560.354	1.030D-23	6.210D-22	4.649D-20
622	290	0330	0220	504.818	546.119	1.060D-23	7.300D-23	1.075D-20
623	99	0110	0000	509.007	538.973	1.010D-23	3.050D-23	1.822D-21
622	130	0310	0200	511.367	547.638	1.020D-23	4.800D-23	3.256D-21
622	300	0310	0220	513.810	556.634	1.030D-23	7.380D-23	1.036D-20
624	90	0200	0110	515.431	543.673	1.020D-23	2.730D-23	1.517D-21
624	162	0220	0110	520.126	538.814	1.040D-23	2.710D-23	3.002D-21
624	156	1000	0000	813.860	875.166	1.040D-23	6.780D-22	4.906D-20
622	193	1000	0000	814.581	892.332	1.040D-23	1.550D-20	1.111D-18
622	346	1110	0110	816.039	881.512	1.060D-23	1.230D-21	1.761D-19
624	212	1110	0110	817.696	861.903	1.020D-23	5.400D-23	7.366D-21
822	91	1000	0000	818.098	855.956	1.010D-23	3.000D-23	1.963D-21
622	149	2000	1000	818.789	878.726	1.020D-23	4.760D-22	3.410D-20
622	120	1200	0200	818.944	868.335	1.020D-23	9.520D-23	6.642D-21
622	242	1220	0220	819.420	868.833	1.050D-23	9.680D-23	1.345D-20
624	76	2000	1000	822.974	857.512	1.010D-23	2.200D-23	1.298D-21
622	193	2110	1110	823.463	865.084	1.010D-23	3.910D-23	5.139D-21
623	125	1000	0000	825.659	876.296	1.030D-23	1.210D-22	8.586D-21
632	132	1000	0000	825.716	878.757	1.090D-23	1.720D-22	1.219D-20
632	104	1110	0110	832.712	862.131	1.010D-23	1.470D-23	1.327D-21
632	108	0200	0000	995.827	1041.270	1.050D-23	5.810D-23	3.977D-21
622	117	1200	1000	1011.934	1060.177	1.020D-23	8.030D-23	5.620D-21
622	181	0200	0000	1016.090	1089.531	1.020D-23	5.200D-21	3.762D-19
624	139	0200	0000	1020.920	1076.013	1.040D-23	2.280D-22	1.652D-20
622	330	0310	0110	1024.174	1089.206	1.010D-23	8.310D-22	1.192D-19
622	88	1310	1110	1026.831	1054.744	1.010D-23	1.320D-23	1.043D-21
623	98	0200	0000	1027.274	1069.094	1.070D-23	4.110D-23	2.732D-21
624	188	0310	0110	1032.101	1073.170	1.060D-23	3.650D-23	4.792D-21
622	125	0400	0200	1034.335	1086.099	1.050D-23	1.290D-22	9.070D-21
622	242	0420	0220	1035.429	1085.395	1.070D-23	9.840D-23	1.369D-20
822	4	0200	0000	1044.894	1046.123	1.010D-23	1.010D-23	4.040D-23
622	106	0510	0310	1048.394	1078.518	1.010D-23	1.490D-23	1.368D-21
622	12	0530	0330	1071.760	1073.903	1.020D-23	1.030D-23	1.230D-22
624	127	2000	0000	1658.640	1709.298	1.040D-23	1.280D-22	9.190D-21
622	274	2110	0110	1664.819	1720.214	1.080D-23	2.320D-22	3.314D-20
622	127	3000	1000	1666.127	1717.887	1.020D-23	1.350D-22	9.604D-21
622	64	2200	0200	1666.918	1699.201	1.050D-23	1.800D-23	9.529D-22
622	173	2000	0000	1667.167	1736.698	1.100D-23	2.920D-21	2.112D-19
622	132	2220	0220	1667.366	1700.475	1.020D-23	1.830D-23	1.977D-21
622	46	3110	1110	1673.349	1695.743	1.010D-23	1.110D-23	4.881D-22
632	90	2000	0000	1679.656	1718.889	1.050D-23	3.250D-23	2.094D-21
623	77	2000	0000	1679.667	1715.075	1.030D-23	2.300D-23	1.369D-21
624	10	2110	0110	1683.758	1685.161	1.010D-23	1.020D-23	1.016D-22
632	101	1200	0000	1835.845	1879.085	1.050D-23	4.720D-23	3.176D-21
622	125	2200	1000	1847.771	1899.112	1.020D-23	1.210D-22	8.591D-21

Table 7
Continued

ISOT ID	LINES	E'	E''	NU.MIN (cm ⁻¹)	NU.MAX (cm ⁻¹)	MIN.I	MAX.I (cm molec ⁻¹)	SUM.I
624	135	1200	0000	1853.758	1907.133	1.080D-23	1.850D-22	1.341D-20
622	146	2310	1110	1855.355	1891.042	1.010D-23	2.150D-23	2.473D-21
622	178	1200	0000	1857.816	1929.897	1.050D-23	4.230D-21	3.063D-19
624	174	1310	0110	1859.962	1898.896	1.030D-23	2.960D-23	3.771D-21
622	320	1310	0110	1860.637	1924.385	1.020D-23	6.740D-22	9.699D-20
622	120	1400	0200	1865.857	1915.483	1.030D-23	9.680D-23	6.802D-21
623	92	1200	0000	1866.427	1906.486	1.020D-23	3.320D-23	2.170D-21
622	226	1420	0220	1867.179	1914.962	1.030D-23	7.380D-23	1.019D-20
622	70	1510	0310	1875.859	1901.457	1.010D-23	1.210D-23	7.838D-22
632	191	0001	0000	1960.682	2037.181	1.030D-23	1.200D-20	8.666D-19
632	338	0111	0110	1963.550	2027.673	1.020D-23	1.020D-21	1.481D-19
632	238	0221	0220	1967.978	2016.194	1.030D-23	8.710D-23	1.217D-20
632	118	0201	0200	1968.943	2017.147	1.020D-23	8.550D-23	6.007D-21
634	153	0001	0000	1972.188	2032.039	1.010D-23	5.240D-22	3.827D-20
632	135	1001	1000	1974.960	2028.988	1.020D-23	1.880D-22	1.352D-20
634	204	0111	0110	1977.717	2019.995	1.020D-23	4.520D-23	6.131D-21
632	120	1111	1110	1982.921	2014.182	1.030D-23	1.670D-23	1.691D-21
822	175	0001	0000	1984.398	2050.390	1.050D-23	2.090D-21	1.561D-19
822	272	0111	0110	1987.753	2039.598	1.020D-23	1.710D-22	2.509D-20
822	96	0221	0220	1996.930	2024.170	1.030D-23	1.380D-23	1.185D-21
622	48	0201	0200	1997.818	2025.051	1.010D-23	1.360D-23	5.819D-22
622	235	0001	0000	1998.474	2092.680	1.110D-23	1.080D-18	7.796D-17
622	528	0111	0110	1999.319	2084.197	1.050D-23	8.550D-20	1.239D-17
822	96	1001	1000	2000.451	2039.521	1.040D-23	3.560D-23	2.409D-21
622	446	0221	0220	2001.043	2074.883	1.100D-23	6.780D-21	9.800D-19
622	183	0201	0200	2001.913	2075.725	1.080D-23	6.620D-21	4.784D-19
622	340	0331	0330	2004.026	2064.517	1.050D-23	5.320D-22	7.680D-20
622	306	0311	0310	2005.659	2065.959	1.090D-23	5.120D-22	7.352D-20
624	207	0001	0000	2008.404	2089.475	1.140D-23	4.720D-20	3.454D-18
622	196	0441	0440	2008.974	2051.569	1.010D-23	4.150D-23	5.428D-21
622	194	1001	1000	2009.730	2087.188	1.050D-23	1.660D-20	1.202D-18
624	406	0111	0110	2009.818	2080.165	1.020D-23	3.760D-21	5.505D-19
622	121	0002	0001	2010.189	2059.412	1.010D-23	9.600D-23	6.778D-21
622	352	1111	1110	2011.485	2077.225	1.010D-23	1.360D-21	1.970D-19
622	190	0421	0420	2011.718	2053.485	1.030D-23	3.940D-23	5.149D-21
624	302	0221	0220	2013.017	2069.371	1.060D-23	2.980D-22	4.326D-20
622	96	0401	0400	2013.184	2054.419	1.050D-23	3.870D-23	2.559D-21
624	143	0201	0200	2013.820	2070.163	1.050D-23	2.930D-22	2.127D-20
623	187	0001	0000	2014.409	2088.595	1.110D-23	8.430D-21	6.150D-19
622	250	1221	1220	2014.951	2065.345	1.040D-23	1.110D-22	1.562D-20
622	123	1201	1200	2015.796	2066.180	1.010D-23	1.090D-22	7.717D-21
623	322	0111	0110	2016.750	2078.457	1.040D-23	6.740D-22	9.747D-20
624	154	0331	0330	2019.515	2055.478	1.010D-23	2.350D-23	2.786D-21
624	158	1001	1000	2020.770	2082.406	1.020D-23	7.660D-22	5.612D-20
624	155	0311	0310	2021.447	2056.885	1.010D-23	2.280D-23	2.727D-21
623	212	0221	0220	2021.689	2065.996	1.020D-23	5.320D-23	7.252D-21
632	126	0400	0000	2021.977	2074.112	1.020D-23	1.290D-22	9.175D-21
623	106	0201	0200	2023.073	2066.844	1.040D-23	5.240D-23	3.586D-21
624	222	1111	1110	2024.810	2069.982	1.050D-23	6.330D-23	8.810D-21
623	127	1001	1000	2028.553	2079.684	1.060D-23	1.340D-22	9.573D-21
622	140	2001	2000	2032.427	2089.395	1.050D-23	2.640D-22	1.903D-20

Table 7
Continued

ISOT ID	LINES	E'	E''	NU.MIN (cm ⁻¹)	NU.MAX (cm ⁻¹)	MIN.I	MAX.I (cm molec ⁻¹)	SUM.I
622	129	1400	1000	2057.617	2110.071	1.120D-23	3.170D-22	2.087D-20
624	44	1400	1000	2063.535	2089.812	1.010D-23	1.330D-23	5.268D-22
822	79	0400	0000	2068.405	2103.222	1.020D-23	2.260D-23	1.383D-21
622	177	0400	0000	2078.977	2151.041	1.090D-23	6.780D-21	4.714D-19
624	137	0400	0000	2079.205	2133.677	1.090D-23	2.960D-22	2.070D-20
623	120	0400	0000	2082.838	2132.100	1.020D-23	9.110D-23	6.453D-21
622	317	0510	0110	2089.493	2153.197	1.040D-23	7.300D-22	1.024D-19
624	177	0510	0110	2093.349	2132.854	1.020D-23	3.210D-23	4.050D-21
622	113	0600	0200	2103.687	2150.694	1.050D-23	8.790D-23	5.933D-21
622	210	0620	0220	2104.817	2149.665	1.070D-23	6.530D-23	8.599D-21
622	131	3000	0000	2521.918	2574.477	1.020D-23	1.520D-22	1.085D-20
622	150	0111	0000	2556.643	2595.252	1.020D-23	7.260D-23	4.975D-21
622	131	2200	0000	2703.381	2756.335	1.060D-23	1.580D-22	1.127D-20
622	144	2310	0110	2706.781	2742.043	1.010D-23	2.080D-23	2.376D-21
632	135	1001	0000	2826.673	2880.701	1.030D-23	1.910D-22	1.369D-20
632	112	1111	0110	2830.158	2860.603	1.020D-23	1.530D-23	1.476D-21
822	94	1001	0000	2837.564	2875.829	1.040D-23	3.330D-23	2.234D-21
622	356	1111	0110	2859.061	2925.604	1.010D-23	1.270D-21	1.878D-19
622	121	1201	0200	2859.542	2909.122	1.020D-23	9.960D-23	7.026D-21
622	242	1221	0220	2859.791	2908.777	1.020D-23	9.520D-23	1.329D-20
622	195	1001	0000	2862.238	2940.324	1.010D-23	1.720D-20	1.244D-18
624	222	1111	0110	2864.091	2909.305	1.020D-23	5.610D-23	7.934D-21
624	157	1001	0000	2864.845	2926.274	1.100D-23	7.500D-22	5.498D-20
622	194	2111	1110	2869.046	2910.490	1.040D-23	3.970D-23	5.264D-21
624	47	2400	1000	2877.018	2906.236	1.010D-23	1.330D-23	5.610D-22
623	127	1001	0000	2879.255	2930.386	1.060D-23	1.350D-22	9.638D-21
624	62	2001	1000	2881.119	2910.543	1.020D-23	1.850D-23	9.446D-22
622	135	2001	1000	2882.011	2936.739	1.070D-23	4.020D-22	2.682D-20
622	115	1400	0000	2916.217	2962.986	1.090D-23	1.530D-22	9.731D-21
632	19	0201	0000	3002.468	3023.786	1.010D-23	1.080D-23	1.989D-22
622	161	0201	0000	3059.953	3124.938	1.080D-23	9.760D-22	7.135D-20
622	59	1201	1000	3062.524	3093.589	1.020D-23	1.620D-23	8.105D-22
622	262	0311	0110	3065.705	3119.916	1.020D-23	1.670D-22	2.375D-20
624	101	0201	0000	3070.441	3112.635	1.030D-23	4.280D-23	2.929D-21
622	82	0401	0200	3074.629	3111.877	1.030D-23	2.580D-23	1.593D-21
622	138	0421	0220	3075.869	3109.915	1.010D-23	1.980D-23	2.197D-21
632	119	0002	0000	3964.167	4012.468	1.020D-23	8.790D-23	6.196D-21
822	57	0002	0000	4012.637	4041.565	1.020D-23	1.530D-23	7.563D-22
622	316	0112	0110	4042.259	4103.583	1.050D-23	6.290D-22	9.058D-20
622	206	0222	0220	4043.416	4087.231	1.020D-23	4.960D-23	6.677D-21
622	185	0002	0000	4043.823	4118.004	1.130D-23	7.900D-21	5.728D-19
622	104	0202	0200	4045.953	4089.098	1.020D-23	4.880D-23	3.312D-21
624	146	0002	0000	4059.312	4115.931	1.010D-23	3.460D-22	2.523D-20
622	125	1002	1000	4060.495	4111.182	1.040D-23	1.220D-22	8.659D-21
624	170	0112	0110	4061.499	4098.707	1.040D-23	2.760D-23	3.486D-21
623	110	0002	0000	4070.802	4115.588	1.030D-23	6.210D-23	4.314D-21

Total number of updated transitions: 24,547

vibrational levels, including the combination states, have been determined by Weber et al. [150, 151]. Rotational and vibrational l-type doubling cause strong intensity perturbation, which has been taken into account in the determination of the line intensities in the ν_5 , $2\nu_5 \leftarrow \nu_5$, and $\nu_4 + \nu_5 \leftarrow \nu_4$ bands [152]. The absolute uncertainties in the data of these bands are less than 0.0003 cm^{-1} in the frequencies and less than 5% in line intensities.

3.15. C_2H_4 (molecule 25)

In GEISA-97, the whole GEISA-92 content has been replaced by new data for both isotopes of ethylene, $^{12}C_2H_4$ and $^{12}C^{13}CH_4$, coded 211 and 311, respectively. The two main absorption infrared regions have been included.

The 701–1170 cm^{-1} spectral region: The spectrum essentially corresponds to the ν_7 band. Some lines of the ν_4 band and many lines of the ν_{10} band (on the low-frequency side) are also included. Neither hot bands nor isotopomer bands are considered. The spectrum has been calculated on the basis of the analysis of the four interacting states ν_{10} , ν_7 , ν_4 , and ν_{12} . [153–156]. The experimental data essentially are Fourier transform (FT) spectra (5000 lines, accuracy 0.0002 cm^{-1}) and tunable diode laser (TDL) spectra for the very weak lines of ν_{10} below 800 cm^{-1} (1000 lines, accuracy 0.001 cm^{-1}) from Cauuet et al. [154] CO_2 -waveguide laser spectra from Herlemont et al. [157] (9 lines, accuracy 0.00001 cm^{-1}), and CO_2 -laser sideband spectra from Legrand et al. [155] and Rusinek et al. [156] (200 saturation lines, accuracy 10^{-6} cm^{-1}). The corresponding rovibrational analysis yields a statistical agreement with this whole set of data. Note that new spectra taken at the McMath Solar Telescope FT facility by Blass et al. [158] are in excellent agreement with the reported spectrum, but they were not introduced in the fit. Most medium and strong lines at low and moderate J and K_a values are estimated to be good within 10^{-5} – 10^{-6} cm^{-1} , but local perturbations [153, 154] can sensitively reduce this accuracy for some lines.

Intensities are calculated on the basis of the eigenvectors to take into account the heavy mixing of the four interacting states, with an absolute calibration based on the TDL measurements of Ref. [158]. Most line intensities are accurate within $\pm 10\%$ or better.

The air-broadened halfwidth has been fixed to $0.087 \text{ cm}^{-1} \text{ atm}^{-1}$ according to Brannon and Varanasi [159] with no variations with the rotational quanta. The value 0.82 has been adopted for the temperature-dependent coefficient n [159]. A default value of $0.09 \text{ cm}^{-1} \text{ atm}^{-1}$ has been set for the self-broadened halfwidth.

The 2917–3243 cm^{-1} spectral region: The spectrum is related to the strong CH-stretching fundamentals ν_9 and ν_{11} , and two combination bands, $\nu_2 + \nu_{12}$ and $2\nu_{10} + \nu_{12}$, which are about ten times weaker. One hot band ($\nu_9 + \nu_{10} - \nu_{10}$) and the ν_9 and ν_{11} bands of the $^{12}C^{13}C$ species are also included. The spectrum has been generated from two experimental spectra: first, the difference-frequency spectrum of Pine [160] with an accuracy of 0.001 cm^{-1} , and second, FT spectra of Mellau and Klee [161] with an accuracy better than 0.0001 cm^{-1} . The analysis is in progress in a broad collaboration with Fayt et al. [162] and Sartakov et al. [163]. The reported lines correspond to Pine's spectrum [160]. In most cases, their frequencies have been replaced by the more accurate values from Mellau's spectra [161]. About 19% (1393) of Pine's lines remain unassigned; they generally correspond to rather weak lines of some hot bands, but some of them probably belong to weak vibrational transitions or to isotopomer bands. At room temperature, the sum of their intensities corresponds to 5% of the integrated intensity in this region. Lines with

Table 8
Summary of GEISA-97 C₂H₄ content

IDENT.	LINES	E'	E''	NU.MIN cm ⁻¹	NU.MAX cm ⁻¹	MIN.I cm molec ⁻¹	MAX.I cm molec ⁻¹	SUM.I cm molec ⁻¹
211	1109	v ₁₀	GROUND	701.203	1076.147	2.650E-23	3.360E-21	2.099E-19
211	4133	v ₇	GROUND	815.558	1170.023	2.660E-23	8.410E-20	1.226E-17
211	574	v ₄	GROUND	825.967	1093.211	2.650E-23	4.010E-21	1.484E-19
211	1393			2917.504	3221.594	2.360E-23	3.640E-21	2.889E-19
211	1538	v ₁₁	GROUND	2919.747	3052.643	6.940E-26	8.960E-21	1.829E-18
211	2882	v ₉	GROUND	2941.821	3242.172	3.390E-25	1.090E-20	3.115E-18
211	600	v ₂ +v ₁₂	GROUND	3026.685	3118.409	1.750E-23	2.180E621	2.874E-19
211	326	2v ₁₀ +v ₁₂	GROUND	3053.482	3140.631	2.800E-23	2.300E-21	1.148E-19
211	142	v ₉ +v ₁₀	v ₁₀	3060.521	3177.173	2.300E-23	1.770E-21	1.978E-20
311	127	v ₁₁	GROUND	2947.832	3011.116	5.060E-24	9.100E-22	1.204E-20
311	154	v ₉	GROUND	3021.669	3180.238	2.910E-23	1.620E-21	2.325E-20
Total number of updated transitions:				12,978				

multiple assignments were divided into their components, with frequency adjustments when possible, and with intensity sharing. Line intensities are generally taken directly from Pine's spectra [161, 164], the absolute accuracy of which is in the range of 1% for strong and medium lines.

The comments on the line widths for the 1000 cm⁻¹ region are also valid for the 3000 cm⁻¹ region.

The new GEISA-97 C₂H₄ data are summarized in Table 8, where the fundamentals of ethylene are numbered according to Herzberg's convention [165]. The isotope code identification (IDENT) is given in column 1 and the number of lines (LINES) for each isotope and transition in column 2; the upper (E') and lower (E'') transition level identifications are in columns 3 and 4 respectively (GROUND stands for the ground level identification), columns 5 and 6 list the minimum (NU.MIN) and maximum (NU.MAX) wavelength values (in cm⁻¹) for each transition; the minimum (MIN.I) and maximum (MAX.I) values for the related intensities (in cm molecule⁻¹) are in columns 7 and 8, respectively, and the intensities sum (SUM.I) value (in cm molecule⁻¹) in column 9.

3.16. H₂O₂ (molecule 35)

Hydrogen peroxide (H₂O₂) is a reservoir molecule of HO_x species in the stratosphere. GEISA-97 involves the microwave to far-infrared and the 7.9 μm regions. Actually, the far-infrared region is commonly used for stratospheric retrievals of this molecule, and significant deficiencies were pointed out by Chance et al. [166] for the available line parameters for this spectral region in GEISA-92. For these reasons, an update was performed for this region which corresponds to the torsion-rotation band of H₂O₂. Using various set of infrared data obtained from Fourier transform spectra, the synthetic spectrum which was generated for this torsion-rotation band takes explicitly into account the perturbations due to the large amplitude torsion motion of the OH bond relative to the OO bond [167–169].

As for the line positions, the calculation takes into account the {Δ(n) = ± 1, Δ(Ka) = ± 2} torsion-rotation resonances, the “staggering” effect which is due to tunneling through the Cis barrier and the vibration–torsion–rotation resonances which involve levels belonging to the ground and to the v₃ = 1 vibrational states. Also, the sinusoidal dependence of the dipole moment

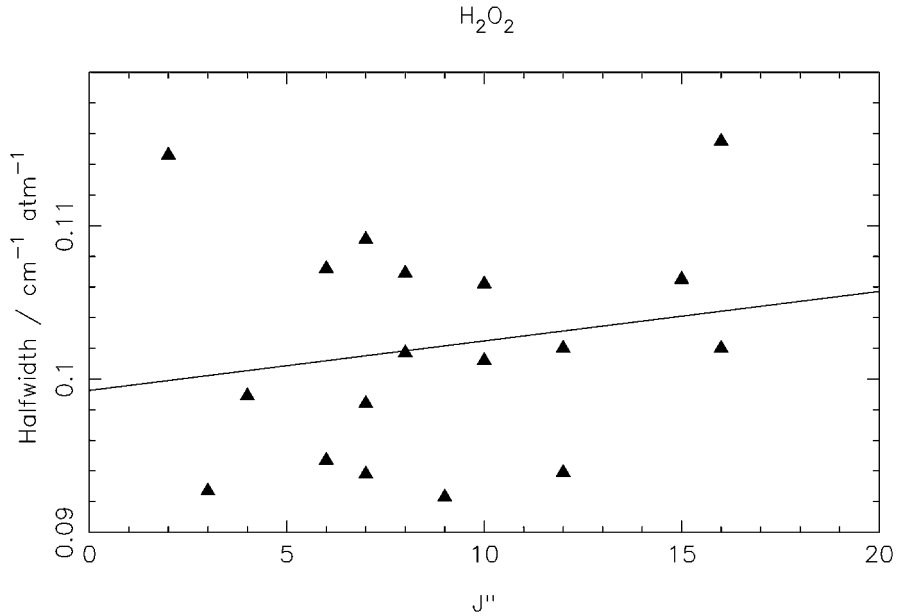


Figure 1. Linear fit in J'' to halfwidths of H_2O_2 .

due to the torsion of OH relative to OO was considered for the intensity calculations. The final linelist involves transitions belonging to 25 different torsional subbands: a detailed description of the linelist is given in Ref. 169.

Data for the air-broadening halfwidths of H_2O_2 are based on the data of Malathy Devi et al. [170] who reported 18 measurements for transitions from $J'' = 3$ to 15. Since data are needed for many other transitions, the data of Ref. [170] are used to predict other values. There is much variation in the data which should be reproduced. However, there are not enough data to fit a polynomial in J'' or to average the halfwidth as a function of J'' . The data were fit to a straight line as a function of J'' , see Fig. 1, to yield the following formula:

$$\gamma(\text{cm}^{-1}/\text{atm}) = 0.099057 + 3.7703 \times 10^{-4} \times J'' \quad (1)$$

The air-broadened halfwidths for transitions of hydrogen peroxide are then determined using Eq. (1).

3.17. H_2S (molecule 36)

The line parameters for the bands between 2142 and 4063 cm^{-1} were included in GEISA-97 the first time. Six bands arising from the ground state ($2\nu_2$, ν_1 , ν_3 , $3\nu_2$, $\nu_1 + \nu_2$ and $\nu_2 + \nu_3$) were predicted for all three isotopes $H_2^{32}S$, $H_2^{33}S$, $H_2^{34}S$, coded 121, 131 and 141, respectively. These calculated values were based on the analysis of positions and intensities by Brown et al. [171], who modeled upper state levels from 0.0004 cm^{-1} for the main isotope to $\pm 0.0006 \text{ cm}^{-1}$ for the $H_2^{33}S$ isotope.

Table 9
Summary of H₂S GEISA-97 updates

ISOT ID	LINES	E'	E''	NU.MIN (cm ⁻¹)	NU.MAX (cm ⁻¹)	MIN.I (cm molec ⁻¹)	MAX.I (cm molec ⁻¹)	SUM.I
121	1147	020	000	2142.835	2852.142	8.110D-26	2.070D-22	1.336D-20
121	1431	001	000	2181.481	3024.778	8.070D-26	8.670D-23	4.842D-21
141	548	020	000	2190.622	2709.642	8.210D-26	9.160D-24	5.799D-22
121	300	030	010	2195.294	2601.428	8.080D-26	1.930D-24	1.116D-22
131	291	020	000	2215.145	2649.630	8.100D-26	1.690D-24	9.744D-23
121	1225	100	000	2224.024	3033.307	8.060D-26	3.610D-22	1.824D-20
141	497	001	000	2327.424	2903.521	8.070D-26	3.920D-24	1.939D-22
141	523	100	000	2378.940	2914.598	8.140D-26	1.600D-23	7.948D-22
131	130	001	000	2426.454	2812.209	8.070D-26	7.210D-25	2.211D-23
131	292	100	000	2467.749	2851.615	8.080D-26	2.960D-24	1.383D-22
121	22	011	010	2484.826	2733.371	8.150D-26	4.710D-25	3.248D-24
121	157	110	010	2552.918	2785.329	8.220D-26	1.140D-24	4.475D-23
121	853	030	000	3303.930	4165.158	2.040D-26	1.810D-23	1.221D-21
121	199	040	010	3326.281	3858.254	2.030D-26	3.850D-25	1.403D-23
141	366	030	000	3344.994	4076.982	2.040D-26	8.030D-25	5.233D-23
121	1860	011	000	3384.726	4245.934	2.050D-26	1.830D-21	1.157D-19
131	153	030	000	3394.438	4024.340	2.020D-26	1.480D-25	7.654D-24
121	1733	110	000	3420.955	4256.547	2.030D-26	1.270D-21	7.339D-20
141	1123	011	000	3490.204	4157.209	2.080D-26	7.970D-23	5.121D-21
141	1025	110	000	3508.978	4171.176	2.020D-26	5.620D-23	3.263D-21
121	708	021	010	3527.312	4060.474	2.030D-26	1.120D-23	7.075D-22
121	604	120	010	3545.595	4063.243	2.020D-26	7.370D-24	4.461D-22
131	807	011	000	3551.116	4098.234	2.020D-26	1.490D-23	9.451D-22
Total number of updated transitions: 16,731								

Intensities of the main isotope were fitted to $\pm 2.5\%$. For the prediction, the calculated intensities were multiplied by the corresponding isotopic abundances of 0.95, 0.0078 and 0.0422 for H₂³²S, H₂³³S, H₂³⁴S, respectively. In addition, six hot bands arising from the ν_2 state were included for the main isotope. The upper-state levels for hot bands in the 3300–4260 cm⁻¹ region were taken from the work of Bykov et al. [172] and band strengths were estimated from laboratory data to $\pm 15\%$.

Air- and self-broadened halfwidths were set to 0.15 and 0.17 cm⁻¹ atm⁻¹, respectively, with the temperature dependence coefficient set to 0.75 for all transitions. The air-broadened width was based on the measurements of Waschull et al. [173] but more recent measurements by Meusel et al. [174] from the same group, indicate that the widths vary as a function of J and this should be considered in future updates. The self-broadened widths were based on both the Ref. [173] study and unpublished results taken from the data of Ref. [171].

The improvements on the GEISA-97 H₂S contents, since GEISA-92, are summarized in Table 9. Column 1 lists the isotopes identification codes (ISOT ID) and column 2 the number of lines (LINES) existing in the spectral interval corresponding to the upper vibrational state E' (column 3) and the lower vibrational state E'' (column 4). The upper and lower vibrational states are identified as ν_1 , ν_2 , ν_3 . In columns 5 and 6 are the minimum (NU.MIN) and the maximum (NU.MAX) frequencies (cm⁻¹) in the actual spectral interval. The related minimum (MIN.I) and maximum (MAX.I) intensity

values are in columns 7 and 8, respectively, and the total line intensities sum (SUM.I) in column 9, in cm molecule^{-1} .

A total of 24 rovibrational bands have been updated or newly introduced in GEISA-97. This corresponds to 16 731 entries (H_2S whole content: 20 788 entries).

3.18. ClONO_2 (molecule 42)

In GEISA-92, absorption parameters for chlorine–nitrate (ClONO_2) were available only as cross-sections, taken from the data of Ballard et al. [175] as detailed in Massie and Goldman [176]. The covered spectral range was: $740\text{--}840 \text{ cm}^{-1}$ (ν_3, ν_4), $1240\text{--}1340 \text{ cm}^{-1}$ (ν_2), and $1680\text{--}1790 \text{ cm}^{-1}$ (ν_1), at 213 and 296 K. In GEISA-97, ClONO_2 has been introduced as a new molecule (numbered 42) in the main molecular line list. It should be noticed that the cross-sections description of ClONO_2 , in the spectral range $1265\text{--}1325 \text{ cm}^{-1}$, has been kept from GEISA-92 (see Section 4).

A new spectroscopic line parameters limited set has been generated for isotopes coded 564 and 764, corresponding to species $^{35}\text{ClONO}_2$ and $^{37}\text{ClONO}_2$, respectively, for bands ν_4 at 780.22 cm^{-1} ($^{35}\text{ClONO}_2$) and 778.87 cm^{-1} ($^{37}\text{ClONO}_2$), and for the band $\nu_4 + \nu_9 - \nu_9$ at 778.74 cm^{-1} ($^{35}\text{ClONO}_2$), as described by Goldman et al. [177]. The line positions are based on the spectroscopic constants of Bell et al. [178] with intensity cutoff for each band of 5×10^{-3} from the maximum intensity and $K_{\text{max}} = J_{\text{max}} = 74$.

The relative band intensities are normalized, by spectral least-squares fitting to a University of Denver laboratory spectrum, and absolute intensities normalized to Ballard et al. [175] values, with the continuum removed.

The air-broadening and self-broadening halfwidths have been set to a uniform value of 0.14 and $0.8 \text{ cm}^{-1} \text{ atm}^{-1}$ at 296 K, with temperature-dependent coefficient of 0.5.

A detailed summary of the ClONO_2 line parameters in GEISA-97 is provided in Table 10. The isotope code identification is given in column 1 and the number of lines for each isotope and transition in column 2; the upper and lower transition level identifications are in columns 3 and 4; columns 5 and 6 list the minimum and maximum wavelength values (in cm^{-1}) for each transition; the minimum and maximum values for the related intensities (in cm molecule^{-1}) are in columns 7 and 8 respectively with the intensities sum value (in cm molecule^{-1}) in column 9, as well.

While the fine structure observed in the ClONO_2 laboratory spectra is not fully accounted for yet, these line parameters provide reliable quantification of ClONO_2 in high-resolution solar absorption spectra from ground-based, air-borne and space-borne spectrometers, by using the 780 cm^{-1} microwindow, similar to that described in Refs. [177, 179] assuming that the continuum is removed in the analysis.

Table 10
Summary of GEISA-97 ClONO_2 content

Ident	#Lines	E'	E''	Nu.Min cm^{-1}	Nu.Max cm^{-1}	Min.I cm.molec^{-1}	Max.I cm.molec^{-1}	Sum.I cm.molec^{-1}
564	10 493	$\nu_4 + \nu_9$	ν_9	763.641	797.741	1.25E-24	2.49E-22	9.19E-19
564	11 495	ν_4	GROUND	766.150	792.488	1.93E-24	3.85E-22	1.44E-19
764	10 211	ν_4	GROUND	765.212	790.805	6.34E-25	1.26E-22	4.66E-19
Total lines:		32 199						

Detailed information on recent results not yet incorporated into the GEISA database is provided in Ref. [180] along with ongoing studies and needs for improvements.

4. GEISA-97 database cross-sections file and associated management software

4.1. Cross-sectional data

Since the beginning of industrialization, the atmosphere has been increasingly influenced by the emission of manmade gases. In particular, the world-wide use, until recently, of the chlorofluorocarbons (freons), especially CCl_3F (CFC11) and CCl_2F_2 (CFC12), resulted in a rapid increase in their concentrations in the atmosphere [181]. The photodecomposition process in the stratosphere frees up Cl atoms that participate in the catalytic destruction of stratospheric ozone [182]. In addition to this effect, these compounds absorb infrared radiation in the region from 700 to 1300 cm^{-1} , lying between the nearly opaque regions due to the infrared absorption by CO_2 and H_2O . As a result of the freons significant absorption, their trace quantities (ranging from 1 to 100 ppm) may contribute significantly to global surface warming [182–184].

The partially halogenated hydrochlorofluorocarbons (HCFCs) and hydrofluorocarbons (HFCs) were found to have the same physical properties as CFCs and to be environmentally more acceptable compounds, regarding their ozone-depletion potential. These gases can be identified as replacement compounds for the industrial use of the CFCs. On the other hand, the HCFCs and HFCs gases are greenhouse ones due to their strong absorption bands located in the IR window [185]. Consequently, because of their atmospheric spectroscopic interest, these compounds have been introduced in the GEISA-97 cross-sections file. In this file, the spectroscopic parameters related to heavy molecules, like the CFCs, are not stored following the usual standard (i.e. via, line frequency, intensity, halfwidth, etc.), but principally as absorption cross-sections determined through the following expression:

$$\sigma(\omega) = \frac{\ln[I_0(\omega)/I(\omega)]}{nl}, \quad (2)$$

where ω is a frequency (cm^{-1}); $\sigma(\omega)$ is the absorption cross-section ($\text{cm}^2 \text{ molecule}^{-1}$); $I_0(\omega)$ and $I(\omega)$ are the intensities, at the frequency ω , of the incident and transmitted radiation, respectively; n is the concentration of the molecules (molecule cm^{-3}); and l the optical path length (cm). It is the $\sigma(\omega)$ value derived from high-resolution experimental data that is cataloged in the GEISA cross-sections file.

Since GEISA-92, the GEISA-97 cross-sections file has been significantly updated and extended. The data on CFC13, CFC14, CFC113, CFC114 and CFC115 [186, 187] have been kept from GEISA-92, and the CFC12 existing data [186, 187] removed. New cross-sections have been cataloged for the following compounds: CFC11 [188]; CFC12 [189]. HCFC22 ([185, 190]; HCFC123, HCFC124, HFC125, HFC134a, HCFC141b, HCFC142b, HFC152a, HCFC225ca, and HCFC225cb [185]; HFC32 and HFC143a [191, 192]; HFC134 [192]; N_2O_5 [193]; SF_6 [190]; ClONO_2 [194]. This represents a total of 23 molecules in the spectral range 556.380–1763.642 cm^{-1} .

The GEISA-97 cross-sections file content informations are summarized in Table 11. In the first column are listed the molecules included with their name (for the CFCs) and corresponding chemical formula; columns 2 and 3 provide the cross-sections spectral intervals availability and temperature conditions; the related author references are in column 4. It should be noted that, for the majority of the molecules, the database comprises cross-sections for a set of temperatures and pressures corresponding to layers of the US standard atmosphere models, that allows simulations of the radiation propagation along slant paths in the atmosphere. Usually, the cross-sections are provided at uniform frequency steps for a given molecule, as is the case of the data listed in Table 11, except for the ones of Refs. [188–190], which are not given on uniform cm^{-1} net steps. They were recorded for different conditions of P, T at different resolutions, with corresponding different step sizes.

Table 12, partitioned by molecule, lists the whole contents of the GEISA-97 cross-sections file. Each of the 23 molecules name and corresponding code for the management of the cross-sections database (see text below) are given in column 1. The atmospheric conditions, temperature (T) in K and pressure (P) in Pa, are listed in columns 2 and 3, respectively. For a given couple, T and P : the fourth column gives the number of available cross-sections (LINES), columns 5 and 6 list the minimum (NU.MIN) and maximum (NU.MAX) frequency (cm^{-1}) values, and columns 7 and 8, the corresponding minimum (MIN.I) and maximum (MAX.I) cross-sections values ($\text{cm}^2 \text{molecule}^{-1}$), respectively. Note that if the pressure is set to zero, it means, in the case of HFC32, 125, 134, 134a, 143a, 152a, HCFC22, 123, 124, 141b, 142b, 225ca, 225cb that the cross-sections have been measured for a pure vapor (non-air broadened) at different pressures for the same point; for CFC13, CFC14, CFC113, CFC114, CFC115, it means that the pure vapor cross-sections were extrapolated to zero pressure from a set of Laboratory data. The total number of available cross-sections of the related molecule is given at the bottom of each corresponding sub-table.

New results [195] on CFC's cross-sections have been obtained beyond this issue of the database and will be included in the next issue of GEISA. These new data provide an extension of the number of temperature and pressure conditions (more than 50, including polar) for CFC11 and CFC12, and also new results for CF_4 and CCl_4 at more than 50 temperature and pressure conditions (including polar).

4.2. Management software

The current version of the GEISA-97 cross-sections database contains 4,716,743 entries related to the 23 molecules listed in Table 11. There are two equivalent versions of this database, one designed for main frame systems [4] and the other one for IBM-PC compatibles [5, 196, 197]. The main frame UNIX version of the cross-sections file occupies 127,352,061 bytes on the hard disk and the IBM-PC version 47,167,430 bytes due to the use of an internal compression format for the data representation.

Examples of the direct image of the GEISA-97 cross-sections file line records are given in Table 13. For each of the listed entries is provided the FORTRAN format of: the wavenumber, ω (cm^{-1}), in column one; the absorption cross-section value, $\sigma(\omega)$ ($\text{cm}^2 \text{molecule}^{-1}$), in column 2; the code M of the molecule (see Table 12), in column 3 and the code C related to the atmospheric conditions (T and P), in column 4. There is a total of 108 atmospheric condition codes.

Table 11
Description of the GEISA-7 cross-sections database

Molecule Formula	Spectral intervals	Temperatures	References
CFC11 CCl ₃ F	810 - 1120 cm ⁻¹	At 11 temperatures from 201 to 296 K	Li and Varanasi ¹⁸⁸
CFC12 CCl ₂ F ₂	850 - 1200 cm ⁻¹	At 15 temperatures from 201 to 296 K	Varanasi and Nemtchinov ¹⁸⁹
CFC13 CClF ₃	765 - 1235 cm ⁻¹	At 6 temperatures from 203 to 293 K	GEISA-92 ^{4,5} Massie et al ¹⁸⁶ McDaniel et al ¹⁸⁷
CFC14 CF ₄	1255-1290 cm ⁻¹	At 6 temperatures from 203 to 293 K	GEISA-92 ^{4,5} Massie et al ¹⁸⁶ McDaniel et al ¹⁸⁷
HCFC22 CHClF ₂	750 - 870 cm ⁻¹ 765 - 1380 cm ⁻¹	At 8 temperatures from 216 to 294 K	Varanasi et al ¹⁹⁰ Clerbaux et al ¹⁸⁵
HFC32 CH ₂ F ₂	995 - 1475 cm ⁻¹	At 9 temperatures from 203 to 297 K, and foreign gas pressure combinations	Smith et al ¹⁹¹
CFC113 C ₂ Cl ₃ F ₃	780 - 1232 cm ⁻¹	At 6 temperatures from 203 to 293 K	GEISA-92 ^{4,5} Massie et al ¹⁸⁶ McDaniel et al ¹⁸⁷
CFC114 C ₂ Cl ₂ F ₄	815 - 1286 cm ⁻¹	At 6 temperatures from 203 to 293 K	GEISA-92 ^{4,5} Massie et al ¹⁸⁶ McDaniel et al ¹⁸⁷
CFC115 C ₂ ClF ₅	955 - 1260 cm ⁻¹	At 6 temperatures from 203 to 293 K	GEISA-92 ^{4,5} Massie et al ¹⁸⁶ McDaniel et al ¹⁸⁷
HCFC123 CHCl ₂ CF ₃	740 - 1450 cm ⁻¹	At 3 temperatures : 253, 270, and 287 K	Clerbaux et al ¹⁸⁵
HCFC124 CHClFCF ₃	675 - 1430 cm ⁻¹	At 287 K (pure vapour)	Clerbaux et al ¹⁸⁵
HFC125 CHF ₂ CF ₃	700 - 1465 cm ⁻¹	At 287 K (pure vapour)	Clerbaux et al ¹⁸⁵
HFC134 CF ₂ HCF ₂ H	600 - 1700 cm ⁻¹	At 6 temperatures from 203 to 297 K and 3 foreign gas pressures	Smith et al ¹⁹²
HFC134a CFH ₂ CF ₃	815 - 1485 cm ⁻¹	At 3 temperatures : 253, 270, and 287 K	Clerbaux et al ¹⁸⁵
HCFC141b CH ₃ CCl ₂ F	710 - 1470 cm ⁻¹	At 3 temperatures : 253, 270, and 287 K	Clerbaux et al ¹⁸⁵
HCFC142b CH ₃ CClF ₂	650 - 1470 cm ⁻¹	At 3 temperatures : 253, 270, and 287 K	Clerbaux et al ¹⁸⁵
HFC143a CF ₃ CH ₃	580 - 1500 cm ⁻¹	At 6 temperatures from 203 to 297 K and 3 foreign gas pressures	Smith et al ¹⁹²
HFC152a CH ₃ CHF ₂	840 - 1490 cm ⁻¹	At 3 temperatures : 253, 270, and 287 K	Clerbaux et al ¹⁸⁵
HCFC225ca CHCl ₂ CF ₂ CF ₃	695 - 1420 cm ⁻¹	At 3 temperatures: 253, 270, and 287 K	Clerbaux et al ¹⁸⁵
HCFC225cb CClF ₂ CF ₂ CHClF	715 - 1375 cm ⁻¹	At 3 temperatures: 253, 270, and 287 K	Clerbaux et al ¹⁸⁵
N ₂ O ₅	557 - 1763 cm ⁻¹	At 4 temperatures from 233 to 293 K	Massie et al ¹⁹³
SF ₆	925 - 955 cm ⁻¹	At 4 temperatures from 216 to 295 K	Varanasi et al ¹⁹⁰
ClONO ₂	1265 - 1325 cm ⁻¹	At 3 temperatures from 201 to 222 K	Orphal et al ¹⁹⁴

Table 12
 GEISA-97 cross-sections database contents. Spectral region: 556.380–1763.642 cm⁻¹

MOL. Code 11	T	P	LINES	NU.MIN	NU.MAX	MIN.I	MAX.I
CFC11	296.0	1.013E+05	11537	810.0056	1119.9951	2.017E-23	4.690E-18
CFC11	283.8	9.466E+04	11371	810.0056	1119.9951	1.160E-23	4.893E-18
CFC11	283.8	8.133E+04	11244	810.0056	1119.8625	1.547E-23	4.864E-18
CFC11	283.9	6.946E+04	11393	810.0056	1119.9951	7.737E-24	4.905E-18
CFC11	272.5	1.013E+05	11566	810.0056	1119.9951	2.228E-23	4.978E-18
CFC11	272.5	8.799E+04	11494	810.0056	1119.9951	1.856E-23	4.992E-18
CFC11	272.5	7.333E+04	11315	810.0056	1119.9830	1.856E-23	5.088E-18
CFC11	272.5	6.133E+04	11387	810.0056	1119.9951	1.114E-23	5.119E-18
CFC11	260.6	8.733E+04	11471	810.0056	1119.9951	1.065E-23	5.294E-18
CFC11	260.6	7.333E+04	11465	810.0056	1119.9951	3.551E-24	5.365E-18
CFC11	260.6	6.000E+04	11471	810.0056	1119.9951	7.102E-24	5.410E-18
CFC11	260.6	4.666E+04	11230	810.0056	1119.9830	2.841E-23	5.471E-18
CFC11	245.7	5.933E+04	11372	810.0056	1119.9951	3.013E-23	5.722E-18
CFC11	245.7	4.746E+04	11342	810.0056	1119.9951	1.339E-23	5.828E-18
CFC11	245.7	3.853E+04	11321	810.0056	1119.9951	1.004E-23	5.894E-18
CFC11	232.7	4.480E+04	11290	810.0056	1119.9348	1.268E-23	6.212E-18
CFC11	232.7	3.333E+04	11250	810.0056	1119.9348	4.439E-23	6.281E-18
CFC11	233.1	2.640E+04	10012	809.9975	1119.9187	1.588E-23	6.460E-18
CFC11	225.8	2.306E+04	10432	809.9975	1119.9991	9.230E-24	6.631E-18
CFC11	225.8	1.733E+04	10378	809.9975	1119.9991	1.231E-23	6.799E-18
CFC11	225.8	1.333E+04	10303	809.9975	1119.9991	1.231E-23	6.946E-18
CFC11	225.8	9.333E+03	40601	810.0009	1119.9991	3.077E-24	7.091E-18
CFC11	225.8	5.333E+03	40210	810.0009	1119.9991	3.077E-24	7.807E-18
CFC11	216.2	2.306E+04	10158	809.9975	1119.9991	8.838E-24	7.069E-18
CFC11	216.1	1.733E+04	9953	809.9975	1119.9857	5.889E-24	7.169E-18
CFC11	216.1	1.333E+04	10009	809.9975	1119.9991	8.834E-24	7.342E-18
CFC11	216.1	9.333E+03	40137	810.0009	1119.9890	2.945E-24	7.955E-18
CFC11	216.1	5.333E+03	40638	810.0009	1119.9991	2.945E-24	8.182E-18
CFC11	208.1	1.333E+04	10228	809.9975	1119.9991	2.836E-24	7.512E-18
CFC11	208.1	9.333E+03	41367	810.0009	1119.9991	2.836E-24	8.311E-18
CFC11	208.1	5.333E+03	40824	810.0009	1119.9991	5.671E-24	8.630E-18
CFC11	201.2	9.333E+03	41176	810.0009	1119.9991	2.741E-24	8.664E-18
CFC11	201.2	5.333E+03	41215	810.0009	1119.9991	8.224E-24	9.099E-18

Total number of cross-sections for CFC11: 601,160

MOL. Code 12	T	P	LINES	NU.MIN	NU.MAX	MIN.I	MAX.I
CFC12	296.3	1.013E+05	24840	850.0032	1199.9904	2.826E-23	1.035E-17
CFC12	284.2	9.333E+04	20676	849.9973	1200.0024	1.394E-23	1.047E-17
CFC12	284.2	7.999E+04	20667	849.9973	1200.0024	2.711E-24	1.067E-17
CFC12	284.2	6.933E+04	20656	849.9973	1200.0024	3.098E-23	1.102E-17
CFC12	273.3	1.013E+05	24871	850.0032	1200.0005	3.128E-23	1.086E-17
CFC12	273.4	8.799E+04	24658	850.0032	1200.0005	7.451E-25	1.373E-17
CFC12	273.4	7.346E+04	24569	850.0032	1200.0005	4.098E-24	1.197E-17
CFC12	273.4	6.133E+04	24521	850.0032	1200.0005	6.705E-24	1.284E-17
CFC12	259.9	8.733E+04	24642	850.0032	1199.9904	7.083E-25	1.249E-17
CFC12	259.9	7.333E+04	24442	850.0032	1199.9904	3.541E-25	1.225E-17
CFC12	259.9	6.000E+04	24276	850.0032	1199.9904	7.083E-25	1.289E-17
CFC12	259.9	4.666E+04	23738	850.0032	1199.9904	8.853E-24	1.411E-17
CFC12	245.5	5.933E+04	24279	850.0032	1199.9904	1.338E-24	1.373E-17
CFC12	245.5	4.733E+04	24039	850.0032	1199.9904	7.359E-24	1.554E-17
CFC12	245.5	3.840E+04	24014	850.0032	1199.9904	3.680E-24	1.576E-17

Table 12
Continued

MOL. Code 12	T	P	LINES	NU.MIN	NU.MAX	MIN.I	MAX.I
CFC12	232.9	4.480E+04	23696	850.0032	1199.9904	2.221E-24	1.634E-17
CFC12	233.1	3.346E+04	24454	850.0032	1199.9904	5.399E-24	1.115E-17
CFC12	232.9	2.626E+04	22989	850.0032	1199.9202	6.347E-25	1.877E-17
CFC12	225.3	2.266E+04	23064	800.0016	1200.0024	2.763E-24	1.979E-17
CFC12	225.3	1.867E+04	19959	849.9973	1200.0024	2.640E-23	2.061E-17
CFC12	225.3	1.347E+04	19618	849.9973	1200.0024	2.456E-24	2.211E-17
CFC12	225.3	9.333E+03	71041	849.9999	1200.0005	6.140E-25	2.400E-17
CFC12	225.3	5.333E+03	67647	849.9999	1199.9971	1.228E-24	2.571E-17
CFC12	216.1	2.280E+04	18333	849.9999	1200.0038	4.711E-24	2.080E-17
CFC12	216.1	1.733E+04	17869	850.0133	1199.9904	7.067E-24	2.250E-17
CFC12	216.1	1.333E+04	18031	850.0133	1200.0038	2.945E-24	2.365E-17
CFC12	216.3	9.333E+03	72228	849.9999	1200.0005	1.768E-24	2.545E-17
CFC12	215.5	5.333E+03	69957	849.9999	1200.0005	5.873E-24	2.786E-17
CFC12	208.2	9.333E+03	70337	850.0233	1200.0005	1.702E-24	2.707E-17
CFC12	201.2	9.333E+03	69124	850.1003	1200.0005	2.741E-24	2.821E-17

Total number of cross-sections for CFC12: 963,235

MOL. Code 13	T	P	LINES	NU.MIN	NU.MAX	MIN.I	MAX.I
CFC13	203.0	0.000E+00	12134	765.0110	1235.2504	0.000E+00	1.187E-17
CFC13	213.0	0.000E+00	12134	765.0110	1235.2504	0.000E+00	1.214E-17
CFC13	233.0	0.000E+00	12134	765.0110	1235.2504	0.000E+00	1.396E-17
CFC13	253.0	0.000E+00	12134	765.0110	1235.2504	0.000E+00	1.060E-17
CFC13	273.0	0.000E+00	12134	765.0110	1235.2504	0.000E+00	1.018E-17
CFC13	293.0	1.013E+05	12134	765.0110	1235.2504	0.000E+00	9.045E-18

Total number of cross-sections for CFC13: 72,804

MOL. Code 14	T	P	LINES	NU.MIN	NU.MAX	MIN.I	MAX.I
CFC14	203.0	0.000E+00	2359	1255.0070	1290.1237	0.000E+00	9.846E-17
CFC14	213.0	0.000E+00	2359	1255.0070	1290.1237	0.000E+00	1.028E-16
CFC14	233.0	0.000E+00	2359	1255.0070	1290.1237	0.000E+00	9.243E-17
CFC14	253.0	0.000E+00	2359	1255.0070	1290.1237	0.000E+00	8.229E-17
CFC14	273.0	0.000E+00	2359	1255.0070	1290.1237	0.000E+00	7.497E-17
CFC14	293.0	1.013E+05	2359	1255.0070	1290.1237	0.000E+00	6.503E-17

Total number of cross-sections for CFC14: 14,154

MOL. Code 22	T	P	LINES	NU.MIN	NU.MAX	MIN.I	MAX.I
HCFC22	216.0	2.357E+04	11032	749.9992	869.9950	1.472E-23	6.921E-18
HCFC22	216.0	5.453E+03	7234	760.0006	859.7167	2.943E-24	1.082E-17
HCFC22	236.0	3.605E+04	9738	760.0006	860.0039	2.251E-23	5.115E-18
HCFC22	240.0	4.112E+04	9748	760.0006	860.0039	3.041E-22	4.488E-18
HCFC22	253.0	0.000E+00	38586	765.0092	1379.9395	2.952E-24	5.029E-18
HCFC22	270.0	0.000E+00	38977	764.9920	1379.9481	1.322E-23	5.019E-18
HCFC22	273.0	7.647E+04	9750	760.0006	860.0039	4.096E-21	3.421E-18
HCFC22	287.0	0.000E+00	37331	764.9920	1379.9050	2.306E-23	4.684E-18
HCFC22	294.0	1.013E+05	8082	760.1442	859.9936	8.012E-24	2.986E-18

Total number of cross-sections for HCFC22: 170,478

Table 12
Continued

MOL. Code 113	T	P	LINES	NU.MIN	NU.MAX	MIN.I	MAX.I
CFC113	203.0	0.000E+00	884	780.4990	1231.9990	4.008E-21	2.512E-18
CFC113	213.0	0.000E+00	884	780.4990	1231.9990	3.102E-21	2.152E-18
CFC113	233.0	0.000E+00	884	780.4990	1231.9990	3.844E-21	1.913E-18
CFC113	253.0	0.000E+00	884	780.4990	1231.9990	2.769E-21	1.710E-18
CFC113	273.0	0.000E+00	884	780.4990	1231.9990	1.909E-21	1.503E-18
CFC113	293.0	1.013E+05	884	780.4990	1231.9990	1.082E-21	1.396E-18
Total number of cross-sections for CFC113: 5,304							

MOL. Code 114	T	P	LINES	NU.MIN	NU.MAX	MIN.I	MAX.I
CFC114	203.0	0.000E+00	24403	815.0010	1285.7302	1.073E-21	3.558E-18
CFC114	213.0	0.000E+00	24403	815.0010	1285.7302	1.442E-20	3.526E-18
CFC114	233.0	0.000E+00	24403	815.0010	1285.7302	1.492E-20	2.811E-18
CFC114	253.0	0.000E+00	24403	815.0010	1285.7302	1.496E-20	2.472E-18
CFC114	273.0	0.000E+00	24403	815.0010	1285.7302	1.177E-20	2.042E-18
CFC114	293.0	1.013E+05	24403	815.0010	1285.7302	6.512E-21	1.874E-18
Total number of cross-sections for CFC114: 146,418							

MOL. Code 115	T	P	LINES	NU.MIN	NU.MAX	MIN.I	MAX.I
CFC115	203.0	0.000E+00	12673	955.0110	1260.3567	7.011E-21	6.092E-18
CFC115	213.0	0.000E+00	12673	955.0110	1260.3567	8.307E-21	5.310E-18
CFC115	233.0	0.000E+00	12673	955.0110	1260.3567	6.373E-21	3.970E-18
CFC115	253.0	0.000E+00	12673	955.0110	1260.3567	0.000E+00	3.752E-18
CFC115	273.0	0.000E+00	12673	955.0110	1260.3567	1.379E-20	3.596E-18
CFC115	293.0	1.013E+05	12673	955.0110	1260.3567	1.449E-20	3.474E-18
Total number of cross-sections for CFC115: 76,038							

MOL. Code 123	T	P	LINES	NU.MIN	NU.MAX	MIN.I	MAX.I
HCFC123	253.0	0.000E+00	55668	739.9905	1448.7539	9.706E-25	2.233E-18
HCFC123	270.0	0.000E+00	59898	739.9905	1449.9506	9.530E-25	2.028E-18
HCFC123	287.0	0.000E+00	61479	740.0077	1449.9850	4.475E-24	1.848E-18
Total number of cross-sections for HCFC123: 177,045							

MOL. Code 32	T	P	LINES	NU.MIN	NU.MAX	MIN.I	MAX.I
HFC32	203.0	1.000E+05	17030	994.9900	1475.0000	1.450E-26	2.116E-18
HFC32	203.0	2.000E+04	20370	995.1255	1475.0000	1.560E-24	3.562E-18
HFC32	203.0	5.000E+03	18837	995.0201	1475.0000	1.680E-24	5.545E-18
HFC32	203.0	0.000E+00	17875	995.2009	1475.0000	4.610E-24	5.706E-18
HFC32	212.0	0.000E+00	17997	994.9900	1475.0000	2.610E-24	5.734E-18
HFC32	222.0	0.000E+00	17875	995.0051	1475.0000	2.190E-24	5.821E-18
HFC32	243.0	0.000E+00	18061	994.9900	1475.0000	3.220E-24	5.868E-18
HFC32	251.0	1.000E+05	19956	995.0352	1475.0000	1.670E-24	2.047E-18
HFC32	251.0	2.000E+04	19790	994.9900	1475.0000	5.100E-25	3.725E-18
HFC32	251.0	5.000E+03	19841	994.9900	1475.0000	6.510E-25	5.306E-18
HFC32	253.0	0.000E+00	18438	994.9900	1475.0000	3.630E-24	5.683E-18

Table 12
Continued

MOL. Code 32	T	P	LINES	NU.MIN	NU.MAX	MIN.I	MAX.I
HFC32	264.0	0.000E+00	17963	995.1406	1475.0000	3.660E-24	5.494E-18
HFC32	287.0	0.000E+00	17512	994.9900	1475.0000	1.680E-24	5.392E-18
HFC32	297.0	1.000E+05	20795	994.9900	1475.0000	6.780E-25	1.996E-18
HFC32	297.0	2.000E+04	20626	994.9900	1475.0000	5.990E-25	3.379E-18
HFC32	297.0	5.000E+03	20001	995.0352	1475.0000	1.143E-23	4.759E-18
HFC32	297.0	0.000E+00	18735	995.0201	1475.0000	1.090E-24	5.186E-18
Total number of cross-sections for HFC32: 321,702							

MOL. Code 124	T	P	LINES	NU.MIN	NU.MAX	MIN.I	MAX.I
HCFC124	287.0	0.000E+00	64294	675.1115	1429.9684	9.932E-25	2.704E-18
Total number of cross-sections for HCFC124: 64,294							

MOL. Code 125	T	P	LINES	NU.MIN	NU.MAX	MIN.I	MAX.I
HFC125	287.0	0.000E+00	57201	699.9915	1464.9824	2.767E-25	3.604E-18
Total number of cross-sections for HFC125: 57,201							

MOL. Code 134	T	P	LINES	NU.MIN	NU.MAX	MIN.I	MAX.I
HFC134a	253.0	0.000E+00	62696	815.0036	1484.0865	4.591E-24	3.970E-18
HFC134a	270.0	0.000E+00	60767	815.0638	1484.9562	6.148E-25	3.769E-18
HFC134a	287.0	0.000E+00	61235	814.9864	1484.9906	1.833E-24	3.220E-18
Total number of cross-sections for HFC134a: 184,698							

MOL. Code 135	T	P	LINES	NU.MIN	NU.MAX	MIN.I	MAX.I
HFC134	203.0	0.000E+00	58399	600.0502	1699.9000	1.180E-24	4.289E-18
HFC134	213.0	0.000E+00	57775	600.0653	1699.9000	3.700E-25	4.285E-18
HFC134	233.0	0.000E+00	57231	599.9900	1699.8247	4.950E-25	4.300E-18
HFC134	253.0	0.000E+00	59904	600.1105	1699.9000	3.630E-25	4.101E-18
HFC134	273.0	0.000E+00	56665	600.0201	1699.8849	9.280E-25	4.006E-18
HFC134	297.0	1.000E+05	62906	599.9900	1699.8096	1.070E-24	3.797E-18
HFC134	297.0	2.000E+04	58029	600.1105	1699.8096	3.930E-25	3.840E-18
HFC134	297.0	5.000E+03	58623	599.9900	1699.7192	6.700E-25	3.851E-18
HFC134	297.0	0.000E+00	60494	599.9900	1699.8397	6.120E-25	3.885E-18
Total number of cross-sections for HFC134 : 530,026							

MOL. Code 141	T	P	LINES	NU.MIN	NU.MAX	MIN.I	MAX.I
HCFC141b	253.0	0.000E+00	53274	709.9869	1469.9845	4.112E-25	4.413E-18
HCFC141b	270.0	0.000E+00	54754	709.9869	1469.9845	2.557E-25	3.910E-18
HCFC141b	287.0	0.000E+00	54392	710.0300	1469.8467	9.151E-26	3.174E-18
Total number of cross-sections for HCFC141b: 162,420							

Table 12
Continued

MOL. Code 142	T	P	LINES	NU.MIN	NU.MAX	MIN.I	MAX.I
HCFC142b	253.0	0.000E+00	54941	649.9895	1474.9865	1.463E-24	5.645E-18
HCFC142b	270.0	0.000E+00	57104	649.9981	1474.9865	5.381E-25	4.964E-18
HCFC142b	287.0	0.000E+00	58070	650.0239	1469.9242	7.200E-25	4.314E-18
Total number of cross-sections for HCFC142b: 170,115							

MOL. Code 143	T	P	LINES	NU.MIN	NU.MAX	MIN.I	MAX.I
HFC143a	203.0	0.000E+00	42978	580.0302	1499.9000	8.770E-25	1.653E-17
HFC143a	213.0	0.000E+00	44400	580.0452	1499.9000	4.130E-25	1.458E-17
HFC143a	233.0	0.000E+00	42796	580.0000	1499.8397	5.020E-25	1.243E-17
HFC143a	253.0	0.000E+00	45601	580.0452	1499.9000	3.940E-25	1.047E-17
HFC143a	273.0	0.000E+00	46567	580.0302	1499.8397	1.600E-24	8.726E-18
HFC143a	297.0	1.000E+05	45774	580.0000	1499.9000	4.290E-25	4.837E-18
HFC143a	297.0	2.000E+04	45183	580.0000	1499.8849	1.090E-24	6.283E-18
HFC143a	297.0	5.000E+03	46775	580.0000	1499.8096	8.940E-25	6.897E-18
HFC143a	297.0	0.000E+00	46012	580.0000	1499.9000	5.160E-25	6.766E-18
Total number of cross-sections for HFC143a: 406,086							

MOL. Code 152	T	P	LINES	NU.MIN	NU.MAX	MIN.I	MAX.I
HFC152a	253.0	0.000E+00	53687	840.0137	1489.9581	1.628E-24	3.416E-18
HFC152a	270.0	0.000E+00	52495	840.0396	1489.9840	2.288E-25	3.193E-18
HFC152a	287.0	0.000E+00	54591	839.9879	1489.9840	8.603E-25	3.016E-18
Total number of cross-sections for HFC152a: 160,773							

MOL. Code 225	T	P	LINES	NU.MIN	NU.MAX	MIN.I	MAX.I
HCFC225ca	253.0	0.000E+00	65746	694.9904	1419.9385	1.982E-24	3.079E-18
HCFC225ca	270.0	0.000E+00	64538	694.9904	1419.9901	3.579E-25	2.973E-18
HCFC225ca	287.0	0.000E+00	66875	695.0077	1419.9901	3.129E-24	2.779E-18
Total number of cross-sections for HCFC225ca: 197,159							

MOL. Code 226	T	P	LINES	NU.MIN	NU.MAX	MIN.I	MAX.I
HCFC225cb	253.0	0.000E+00	70420	714.9890	1374.7566	5.724E-24	2.129E-18
HCFC225cb	270.0	0.000E+00	65472	714.9890	1374.9891	9.824E-25	2.102E-18
HCFC225cb	287.0	0.000E+00	69890	714.9888	1374.9818	3.072E-24	1.857E-18
Total number of cross-sections for HCFC225cb: 205,782							

MOL. Code 201	T	P	LINES	NU.MIN	NU.MAX	MIN.I	MAX.I
CIONO ₂	201.0	0.000E+00	2401	1265.0067	1324.9822	0.000E+00	3.129E-18
CIONO ₂	211.0	0.000E+00	2401	1265.0067	1324.9822	0.000E+00	3.451E-18
CIONO ₂	222.0	0.000E+00	2401	1265.0067	1324.9822	0.000E+00	3.156E-18
Total number of cross-sections for CIONO ₂ : 7,203							

Table 12
Continued

MOL. Code 200	T	P	LINES	NU.MIN	NU.MAX	MIN.I	MAX.I
N ₂ O ₅	233.0	0.000E+00	491	556.8613	1763.1616	1.406E-20	1.973E-18
N ₂ O ₅	253.0	0.000E+00	491	556.8613	1763.1616	1.891E-20	2.017E-18
N ₂ O ₅	273.0	0.000E+00	492	556.3792	1763.1616	1.812E-20	1.987E-18
N ₂ O ₅	293.0	1.013E+05	492	556.3792	1763.1616	2.298E-20	2.015E-18
Total number of cross-sections for N ₂ O ₅ : 1,966							

MOL. Code 202	T	P	LINES	NU.MIN	NU.MAX	MIN.I	MAX.I
SF ₆	215.9	2.266E+04	2988	925.0012	955.0029	3.614E-20	1.101E-16
SF ₆	215.9	1.200E+04	2865	925.0012	955.0029	6.854E-22	1.171E-16
SF ₆	215.9	6.346E+03	2988	925.0012	955.0029	2.091E-19	1.240E-16
SF ₆	215.9	3.373E+03	2910	925.0012	955.0029	4.327E-21	1.283E-16
SF ₆	245.9	4.746E+04	2970	925.0012	955.0029	1.846E-21	7.891E-17
SF ₆	273.4	7.334E+04	2967	925.0012	955.0029	4.955E-22	5.611E-17
SF ₆	294.6	1.014E+05	2988	925.0012	955.0029	6.048E-20	4.504E-17
Total number of cross-sections for SF ₆ : 20,676							

Table 13
Examples of the direct image of the GEISA-97 cross-sections file line records

ω	σ	M	C
1186.00061	5.214E-20	13	85
1186.00061	5.551E-20	13	86
1186.00232	1.062E-20	12	62
1186.00232	1.616E-21	12	56
1186.00232	1.768E-20	12	60
1186.00232	2.302E-20	12	61
1186.00232	4.130E-21	12	63
1186.00305	3.523E-20	134	92
1186.00305	4.819E-20	134	106
1186.00305	5.097E-20	134	103
FORMAT(F10.5, E10.3, I3, I3) corresponding to:			
ω	F10.5	Frequency in cm ⁻¹ (F10.6 if 0 < ω < 1000 cm ⁻¹)	
σ	E10.3	Absorption cross-section in cm ² mol ⁻¹	
M	I3	Molecule identification code	
C	I3	Atmospheric conditions code	

Examples of some of these codes (the complete list is provided with the cross-sections file) are listed in Table 14, where the atmospheric condition codes C are in column one, and the temperature T (in K) and pressure P (in Pa) in columns 2 and 3, respectively.

Table 14

Example of atmospheric condition codes (temperature and pressure values) used in the GEISA-97 cross-sections database. Whole file total number of condition codes: 108

C	T	P
1	296.0	101325.00
2	283.8	94658.88
3	283.8	81326.64
4	283.9	69460.95
5	272.5	101325.00
6	272.5	87992.76
7	272.5	73327.30
8	272.5	61328.29
C - code of atmospheric conditions		
T - temperature in K		
P - pressure in Pa		

For the use and management of the GEISA cross-sections file, two versions of the related software have been developed: the CROSS_U program to be used on the main frame systems and the CROSSUTI.EXE program designed for IBM-PC compatibles. The CROSS_U program allows the user to make extractions, from the whole file, the data being selected by the molecule type and the temperature and pressure experimental conditions. Graphic tools are included in the IBM-PC management software package, for the purpose of displaying selected cross-sections plotting information, as well as of making extraction of selected data. Both programs are equipped with an interactive friendly accessible menu.

To illustrate the plotting facilities of CROSSUTI.EXE, Fig. 2 displays, on the same graphic, in the spectral range $1080\text{--}1150\text{ cm}^{-1}$, the plot of the absorption cross-sections of CFC11 and CFC12, at $P = 1\text{ atm}$ and $T = 296\text{ K}$ [188, 189], HFC32 and HFC134, at $P = 1\text{ atm}$ and $T = 297\text{ K}$ Refs. [191, 192] and HCFC124 and HCFC141b, at a pressure corresponding to pure vapor and $T = 287\text{ K}$ [185].

5. Availability of the GEISA database 1997 version

The current GEISA-97 database, and the former version GEISA-92 as well, are available, with their associated management software, freely from the ARA/LMD group workstations (IBM RISC 6000 or SUN) web site: <http://ara01.polytechnique.fr/registration>

It is possible to extract part of the database on-line using the GEISA associated management software facilities, as described in Refs. [4, 11].

Added to this facility, the GEISA-97 file as a whole, with related description and general information files, are available from the following anonymous ftp site:

ara01.polytechnique.fr

in the subdirectories: pub/geisa

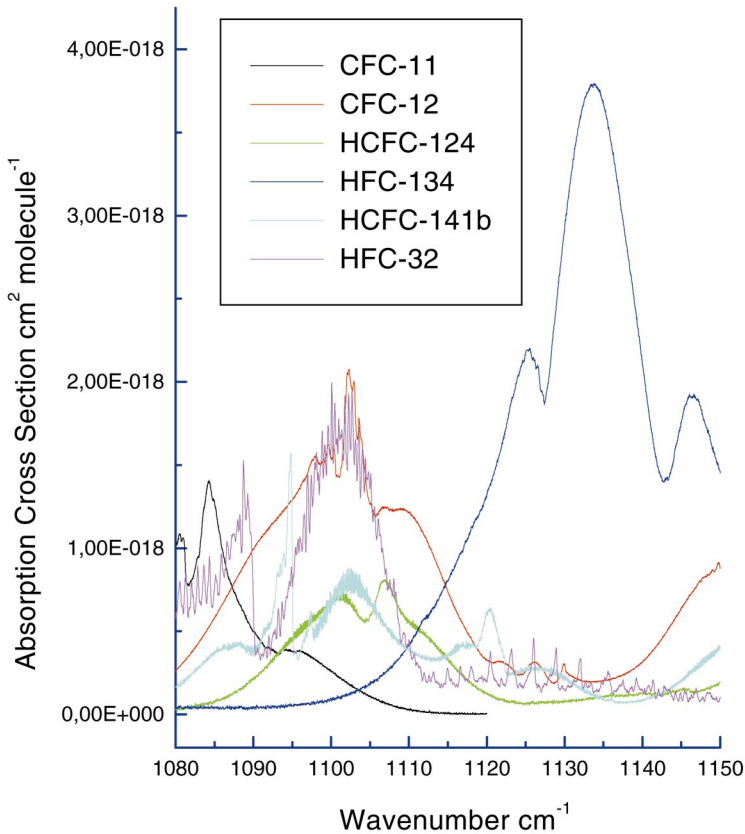


Fig. 2. Illustration of program CROSSUTLEXE plotting facilities. Plot of GEISA97 absorption cross-sections of: CFC11 and CFC12, at $P = 1$ atm and $T = 296$ K (Refs. 188–189), HFC32 and HFC134, at $P = 1$ atm and $T = 297$ K (Refs. 191–192), and HCFC124 and HCFC141b, with a pressure corresponding to pure vapor and $T = 287$ K (Ref. 185).

More complementary information and assistance will be provided upon request at the first author's e-mail address: husson@ara01.polytechnique.fr.

6. Conclusion: examples of GEISA database improvements needed

Many researchers throughout the world are currently making every effort to ensure the quality of the spectroscopic parameters which are needed as input to atmospheric remote-sensing investigation. Several studies, partially overlapping, partially complementary, are currently undertaken. The regularly updated and evolving spectroscopic databases, such as GEISA, still have their limitations and faults, which have to be corrected or improved upon, in order to meet the requirements of a diverse group of users. As an example of actual improvement needs, the following list, established in the frame of the ISSWG (IASI Science Sounding Working Group) activities, provides the IASI soundings spectroscopy enhancement requirements.

6.1. *Quality control of spectroscopic parameters for the most abundant species*

- Need to validate systematically the existing databases (HITRAN, GEISA) for the stronger absorbers: H₂O, CO₂, CH₄, O₃, N₂O.
- Intercomparison of existing databases is not sufficient. Comparison with real atmospheric spectra recorded in well-documented conditions is necessary to locate deficiencies.
- Patches and add-ons can degrade the database consistency (duplicates or missing lines).
- Existing and new laboratory data should be combined in a consistent manner using suitable theoretical models for the calculation of line positions, intensities and widths.
- Coding of uncertainties by an index is insufficient for proper use in the forward model variance-covariance matrix. Better and more realistic errors on spectroscopic parameters are required.

6.2. *Urgent needs*

- Water vapour continuum studies (foreign and self) and temperature dependence.
- Perform long path laboratory measurements.
- Perform real atmospheric measurements along horizontal paths in well-documented conditions.
- Improve existing parameterizations.
- Elaborate new theoretical models.
- Correct known inadequacies observed when modelling high-resolution atmospheric spectra (H₂O, CO₂, CH₄) recorded from the ground, from balloon or from space.

6.3. *Specific recommendations*

6.3.1. *H₂O*

- Weak lines in the regions 650–1200 and 3000–6000 cm⁻¹ especially, still have incorrect positions and intensities. There is a need for both measurements and improved theoretical calculations.
- Widths (foreign and self) have not been validated by enough systematic laboratory work. Very strong variations from line to line exist.
- Temperature dependencies of widths are poorly measured or calculated.
- Pressure shifts can be important in the lower troposphere.
- Some lines recorded at high resolution in ground based solar spectra do show profiles inconsistent with current line shape formalisms.
- More detailed line shape measurements and modelling needed for H₂O (in connection with continuum studies).

6.3.2. *CO₂*

- Validation of line intensities for the isotopomers in ¹³C, ¹⁸O and ¹⁷O needed.
- New line shape studies needed in the 15 μm band (laboratory and theoretical).

6.3.3. *O₃*

- For lower stratospheric and tropospheric ozone retrievals a better knowledge of the temperature dependence of the line widths is needed.

6.3.4. CH_4

- Intensive laboratory and theoretical work still needed for air-broadened widths.
- Line shape studies needed including line interference effects in multiplets and Q branches

6.3.5. HNO_3

HNO_3 has a potential contribution in the IASI spectra (in the window regions). Work on absolute line intensities is still needed.

6.3.6. *Heavy molecules described in terms of cross-section instead of line by line parameters*

- Establish a priority list with the known scenarios for man-made species (CFCs, HCFCs, perfluorinated compounds) based on existing cross-sectional data.
- Perform new measurements and establish smooth parameterizations (as a function of temperature and total pressure) to avoid the use of empirical extrapolations of accurately measured cross-sections as substitutes to unavailable data.

References

- [1] JPL, AIRS Atmospheric Infrared Sounder Science and measurements requirements. JPL Publication, D6665 REV.1 9/91, Jet Propulsion Laboratory, Pasadena, 1991.
- [2] Phulpin T, Chalon G, Courtier P, Cayla FR, Langevin M, Diebel D, Klaes KD, IASI, a new generation atmospheric sounder for the EUMETSAT polar system. In: Eyre JR, editor. Proc IX ITSC, Igl. Austria, 20–26 February 1997, published by ECMWF, Reading, U.K., May 1997;375–89.
- [3] Chédin A, Husson N, Scott NA. Une banque de données pour l'étude des phénomènes de transfert radiatif dans les atmosphères planétaires: la banque "GEISA". Bull. d'Information du Centre de Données Stellaires (France) 1982;22:121.
- [4] Husson N, Bonnet B, Scott NA, Chédin A. Management and study of spectroscopic information: the GEISA program. J. Quantitative Spectrosc Radiative Transfer 1992;48:509–18.
- [5] Husson N, Bonnet B, Chédin A, Scott NA, Chursin AA, Golovko VF, Tyuterev VIG. The GEISA data bank in 1993. A PC/AT compatible computers' new version. J Quantitative Spectrosc Radiative Transfer, 1994;52:425–38.
- [6] Jacquinet-Husson N, Scott NA, Chédin A, Bonnet B, Barbe A, Tyuterev VIG, Champion JP, Winnewisser M, Brown LR, Gamache R, Golovko VF, Chursin A. The GEISA system in 1996: toward an operational tool for the second generation vertical sounders radiance simulation. J Quantitative Spectrosc Radiative Transfer 1998;59:511–27.
- [7] Brown LR, Gunson MR, Toth RA, Irion FW, Rinsland CP, Goldman A. 1995 Atmospheric trace molecule spectroscopy (ATMOS) linelist. Appl. Opt. 1996;35:2828–48.
- [8] Rothman LS, Rinsland CP, Goldman A, Massie ST, Flaud J-M, Perrin A, Dana V, Mandin J-Y, Schroeder J, Mc Cann A, Gamache RR, Wattson RB, Yoshino K, Chance K, Jucks K, Brown LR, Varanasi P. The HITRAN molecular spectroscopic database and HAWKS (HITRAN Atmospheric Workstation). J Quantitative Spectrosc Radiative Transfer 1998;60:665–710.
- [9] Tyuterev VIG, Babikov YuL, Tashkun SA, Perevalov VI, Nikitin A, Champion JP, Hilico JC, Loete M, Pierre CL, Pierre G, Wenger Ch, TDS. Spectroscopic databank for spherical tops. J Quantitative Spectrosc Radiative Transfer 1994;52:459–80.
- [10] Wenger C, Champion, JP, STDS. Spherical Top Data System. A software for the simulation of spherical top spectra. J Quantitative Spectrosc Radiative Transfer 1998;59:471–80.
- [11] Chédin A, Husson N, Scott NA, Cohen-Hallaleh I, Berroir A, The GEISA data bank 1984 version. Internal Note LMD, no. 127, February 1985, reviewed October 1986.

- [12] Rothman LS, Gamache RR, Tipping RH, Rinsland CP, Smith MAH, Chris Benner D, Malathy Devi V, Flaud J-M, Camy-Peyret C, Perrin A, Goldman A, Massie ST, Brown LR, Toth RA, The HITRAN molecular database: editions of 1991 and 1992. *J Quantitative Spectrosc Radiative Transfer* 1992;48:469–507.
- [13] Brown LR, Farmer CB, Rinsland CP, Toth RA. Molecular line parameters for the atmospheric trace molecule spectroscopy experiment. *Appl Opt*, 1987;26:5154–82.
- [14] Husson N, Chédin A, Scott NA, Bailly D, Graner G, Lacombe N, Lévy A, Rossetti C, Tarrago G, Camy-Peyret C, Flaud, J-M, Bauer A, Colmont J-M, Monnanteuil N, Hilico J-C, Pierre G, Loete M, Champion J-P, Rothman LS, Brown LR, Orton G, Varanasi P, Rinsland CP, Smith MAH, Goldman A. The GEISA spectroscopic line parameters data bank in 1984. *Ann Geophys* 1986;4:185–90.
- [15] Rinsland CP, Smith MAH, Malathy Devi V, Perrin A, Flaud J-M, Camy-Peyret, C. The ν_2 bands of $^{16}\text{O}^{17}\text{O}^{16}\text{O}$ and $^{17}\text{O}^{16}\text{O}^{16}\text{O}$: line positions and intensities. *J Mol Spectrosc* 1991;149:474–480.
- [16] Flaud J-M, Camy-Peyret C, Rinsland CP, Smith MHA, Malathy Devi V, Atlas of Ozone Spectral parameters from microwave to medium infrared. 1990, Academic Press, San Diego, CA.
- [17] Barbe A, Plateaux JJ, Bouazza S, Flaud J-M, Camy-Peyret, C. Spectral properties of ozone in the 5 μm region. *J Quantitative Spectrosc Radiative Transfer* 1992;48:599–610.
- [18] Bouazza S, Barbe A, Plateaux JJ, Flaud J-M, Camy-Peyret C, The $3\nu_1$ and $\nu_1 + 3\nu_3 - \nu_2$ absorption bands of $^{16}\text{O}_3$. *J Mol Spectrosc* 1993;160:371–77.
- [19] Birk M, Wagner G, Flaud J-M, Hausamann, D. Line strenghts in the $\nu_3 - \nu_2$ hot band of ozone. *J Mol Spectrosc* 1994;163:262–75.
- [20] Flaud J-M, Camy-Peyret C, Perrin A, Malathy Devi V, Barbe A, Bouazza S, Plateaux JJ, Rinsland CP, Smith MAH, Goldman A. Line parameters for hot bands in the 3.3 μm spectral region. *J Mol Spectrosc* 1993;160:378–86.
- [21] Malathy Devi V, Perrin A, Flaud J-M, Camy-Peyret C, Rinsland CP, Smith MAH. Line positions and intensities for the $\nu_2 + 3\nu_3$ band of $^{16}\text{O}_3$ around 2.7 μm . *J Mol Spectrosc* 1990;143:381–88.
- [22] Perrin A, Vasserot A-M, Flaud J-M, Camy-Peyret C, Malathy Devi V, Smith MAH, Rinsland CP, Barbe A, Bouazza S, Plateaux JJ. The 2.5 μm bands of ozone: line positions and intensities. *J Mol Spectrosc* 1991;149:519–29.
- [23] Barbe A, Plateaux JJ, Bouazza S, Sulakshina O, Mikhaïlenko, S, Tyuterev VIG, Tashkun S, Experimental and theoretical study of absolute intensities of ozone spectral lines in the range 1850–2300 cm^{-1} . *J Quantitative Spectrosc Radiative Transfer* 1994;52:341–55.
- [24] Barbe A, Sulakshina O, Plateaux JJ, Hamdouni A, Bouazza S. High resolution infrared spectra of ozone in the 2300–2600 cm^{-1} region. *J Mol Spectrosc* 1995;170:244–50.
- [25] Barbe A, Mikhaïlenko S, Plateaux JJ, Tyuterev VI G. First study of the $\nu_2 = 3$ dyad $\{(130)(031)\}$ of ozone through the analysis of hot bands in the 2300–2600 cm^{-1} region. *J Mol Spectrosc* 1998;187:70–4.
- [26] Bouazza S, Barbe A, Mikhaïlenko S, Plateaux JJ. Line positions and intensities of the $\nu_1 + 2\nu_2 + \nu_3$ and $2\nu_2 + 2\nu_3$ bands of $^{16}\text{O}_3$. *J Mol Spectrosc* 1994;166:365–71.
- [27] Barbe A, Tyuterev VIG, Mikhaïlenko S. Private communication, 1997.
- [28] Barbe A, Régalia L, Plateaux JJ, Von der Heyden P, Thomas X. Temperature dependence of N_2 and O_2 broadening coefficients of ozone. *J Mol Spectrosc*, 1996;180:175–82.
- [29] Gamache RR. Temperature dependence of N_2 -broadened halfwidths of ozone. *J Mol Spectrosc*, 1985;114:31–41.
- [30] Gamache RR, Rothman LS. Theoretical N_2 -broadened halfwidths of $^{16}\text{O}_3$. *Appl Opt* 1985;24:1651–56.
- [31] Gamache RR, Davies RW. Theoretical N_2 -, O_2 -, and air-broadened halwidths of $^{16}\text{O}_3$ calculated by quantum Fourier transform theory with realistic collision dynamics. *J Mol Spectrosc* 1985;109:283–99.
- [32] Smith, MAH. Private communication, 1990.
- [33] Rinsland, CP. Private communication, 1990.
- [34] Smith MAH, Rinsland CP, Malathy Devi V. Measurements of sel-broadening of infrared absorption lines of Ozone. *J Mol Spectrosc* 1991;147:142–54.
- [35] Johns JWC, Lu Z, Weber M, Sirota JM, Reuter DC. Absolute Intensities in the ν_2 fundamental of N_2O at 17 μm . *J Mol Spectrosc* 1996;177:203–10.
- [36] Weber M, Sirota JM, Reuter DC. l-resonance effects and pressure broadening of N_2O at 17 μm . *J Mol Spectrosc* 1996;177:211–20.

- [37] Maki AG, Wells JS. Wavenumber calibration tables from heterodyne frequency measurements. NIST Special Publication 821, National Institute of Standard and Technology, Gaithersburg, 1991.
- [38] Lacombe N, Levy A, Guelachvili G. Fourier transform measurement of self-, N₂-, and O₂-broadening of N₂O lines: temperature dependence of line widths. *Appl Opt* 1984;23:425–35.
- [39] Margottin-Maclou M, Dahoo P, Henry A, Henry L. Self-broadening parameters in the ν_3 band of $^{14}\text{N}_2^{16}\text{O}$. *J Mol Spectrosc* 1985;111:275–90.
- [40] Henry A, Margottin-Maclou M, Lacombe N, N₂- and O₂-broadening parameters in the ν_3 band of $^{14}\text{N}_2^{16}\text{O}$. *J Mol Spectrosc* 1985;111:291–300.
- [41] Toth RA. Line strengths ($900\text{--}3600\text{ cm}^{-1}$), self-broadened linewidths, and frequency shifts ($1800\text{--}2360\text{ cm}^{-1}$) of N₂O. *Appl Opt* 1993;32:7326–65.
- [42] Brown LR, Loete M, Hilico JC. Line strengths of the ν_2 and ν_4 bands of $^{12}\text{CH}_4$ and $^{13}\text{CH}_4$. *J Mol Spectrosc* 1989;133:273–311.
- [43] Champion JP, Hilico JC, Wenger Ch, Brown LR. Analysis of the ν_2/ν_4 Dyad of $^{12}\text{CH}_4$ and $^{13}\text{CH}_4$. *J Mol Spectrosc* 1989;133:256–72.
- [44] Hilico JC, Champion JP, Toumi S, Tyuterev VIG, Tashkun SA. New analysis of the pentad system of methane and prediction of the (Pentad-Pentad) spectrum. *J Mol Spectrosc* 1994;168:455–76.
- [45] Ouardi O, Hilico JC, Loëte M, Brown LR. The hot bands of methane between 5 and 10 μm . *J Mol Spectrosc* 1996;180:311–322.
- [46] Jouvard JM, Lavorel B, Champion JP, Brown LR. Preliminary analysis of the pentad of $^{13}\text{CH}_4$ from Raman and infrared spectra. *J Mol Spectrosc* 1991;150:201–17.
- [47] Hilico JC, Toumi S, Brown LR. The octad of interacting vibrational states of methane. In: Sauval AJ, Blomme R, Grevesse N, editors. *Laboratory and astrophysical high resolution spectra*. A.S.P. Conf. Ser. San Francisco, 1995;322–4.
- [48] Brown LR, Margolis JS, Champion JP, Hilico JC, Jouvard JM, Loete M, Chackerian Jr C, Tarrago G, Benner DC. Methane and its isotopes: current status and prospects for improvement. *J Quantitative Spectrosc Radiative Transfer* 1992;48:617–28.
- [49] Babikov Yu L, Tyuterev VIG, Wenger C, Champion JP. TDS information system on high resolution spectroscopy of spherical top molecules. *Proc 2nd Int Workshop on Advances in Databases and Information Systems (ADBIS'95)*, vol 2, phasis publishing house, Moscow, June 1995.
- [50] Goldman A, Updated Line parameters for NO X²Π–X²Π(ν'' , ν') transitions. Progress Report, University of Denver, December 1996.
- [51] Goldman A, Brown LR, Schoenfeld WG, Spencer MN, Chackerian Jr C, Giver LP, Rinsland CP, Coudert LH, Dana V, Mandin J-Y. Nitric oxide line parameters: review of 1996 HITRAN update and new results. *J Quantitative Spectrosc Radiative Transfer* 1998;60:825–38.
- [52] Goldman A, Schoenfeld WG, Goorvitch D, Chackerian Jr C, Dothe H, Mélen F, Abrams MC, Selby JEA. Updated line parameters for OH X²Π–X²Π(ν'' , ν') transitions. *J Quantitative Spectrosc Radiative Transfer* 1998;59:453–69.
- [53] Coudert LH, Dana V, Mandin J-Y, Morillon-Chapey M, Farrenq R, Guelachvili G. The spectrum of nitric oxide between 1700 and 2100 cm^{-1} . *J Mol Spectrosc* 1995;172:435–48.
- [54] Goorvitch D, Galant DC. Schrödinger's radial equation: solution by extrapolation. *J Quantitative Spectrosc Radiative Transfer* 1992;47:391–9.
- [55] Chackerian Jr C. Private communication, 1996.
- [56] Spencer MN, Chackerian Jr C, Giver LP, Brown LR. Temperature dependence of nitrogen broadening of the NO fundamental vibrational band. *J Mol Spectrosc* 1997;181:307–15.
- [57] Falcone PK, Hanson RK, Kruger CH. Tunable diode laser measurements of the band strength and collision halfwidths of nitric oxide. *J Quantitative Spectrosc Radiative Transfer* 1983;29:205–21.
- [58] Houdeau JP, Boulet C, Bonamy J, Khayar A, Guelachvili G. Air broadened NO linewidths in a temperature range of atmospheric interest. *J Chem Phys* 1983;79:1634–40.
- [59] Phillips WJ, Walker HC. Nitrogen-broadened linewidths and strengths of nitric oxide utilizing tunable diode laser spectroscopy. *J Chem Phys* 1986;85:3211–6.
- [60] Ballard J, Johnston WB, Kerridge BJ, Remedios JJ. Experimental spectral line parameters in the 1–0 band of nitric oxide. *J Mol Spectrosc* 1988;127:70–82.

- [61] Spencer MN, Chackerian Jr C, Giver LP, Brown LR. The nitric oxide fundamental band: frequency and shape parameters for rovibrational lines. *J Mol Spectrosc*, 1994;165:506–24.
- [62] Pine AS, Maki AG, Chou N-Y. Pressure broadening, lineshapes, and intensity measurements in the $2 \leftarrow 0$ Band of NO. *J Mol Spectrosc* 1985;114:132–47.
- [63] Goldman A, Murcray FJ, Rinsland CP, Blatherwick RD, David SJ, Murcray FH, and Murcray DG. Mt Pinatubo SO₂ column measurements from Mauna Loa. *Geophys Res Lett* 1992;19:183–6.
- [64] Mankin WG, Coffey MT, Goldman A. Airbone observations of SO₂, HCl and O₃ in the stratospheric plume of the Pinatubo volcano in July 1991. *Geophys Res Lett*, 1992;19:179–82.
- [65] Lafferty WJ, Pine AS, Hilpert G, Sams RL, Flaud JM. The $\nu_1 + \nu_3$ and $2\nu_1 + \nu_3$ band systems of SO₂: line positions and intensities. *J Mol Spectrosc* 1996;176:280–6.
- [66] Lafferty WJ, Pine AS, Flaud J-M, Camy-Peyret C. The $2\nu_3$ band of SO₂: line positions and intensities. *J Mol Spectrosc* 1993;157:499–511.
- [67] Bezdard B, de Bergh C, Crisp D, and Maillard JP. The deep atmosphere of Venus revealed by high resolution nightside spectra. *Nature* 1990;345:508–11.
- [68] Lafferty WJ, Fraser GT, Pine AS, Flaud J-M, Camy-Peyret C, Dana V, Mandin J-Y, Barbe A, Plateaux JJ, Bouazza S. The $3\nu_3$ band of ³²S¹⁶O₂: line positions and intensities. *J Mol Spectrosc* 1992;154:51–60.
- [69] Flaud J-M, Lafferty WJ. ³²S¹⁶O₂: a refined analysis of the $3\nu_3$ band and determination of equilibrium rotational constants. *J Mol Spectrosc* 1993;161:396–402.
- [70] Perrin A, Camy-Peyret C, Flaud JM. Infrared nitrogen dioxide in the HITRAN database. *J Quantitative Spectrosc Radiative Transfer* 1992;48:645–52.
- [71] Perrin A, Flaud J-M, Camy-Peyret C, Goldman A, Murcray FJ, Blatherwick RD, Rinsland CP. The ν_2 and $2\nu_2 - \nu_2$ bands of ¹⁴N¹⁶O₂: electron spin-rotation and hyperfine contact resonances in the (010) vibrational state. *J Mol Spectrosc* 1992;160:456–63.
- [72] Malathy Devi V, Das PP, Bano A, Narahari Rao K, Flaud J-M, Camy-Peyret C, Chevillard JP. Diode laser measurements of intensities, N₂ broadening and self broadening coefficients of lines of the ν_2 band of ¹⁴N¹⁶O₂. *J Mol Spectrosc* 1981;88:251–8.
- [73] Perrin A, Flaud J-M, Camy-Peyret C, Vasserot AM, Guelachvili G, Goldman A, Murcray FJ, Blatherwick RD., The $\{\nu_3, 2\nu_2, \nu_1\}$ interacting bands of NO₂: line positions and intensities. *J Mol Spectrosc*, 1992;154:391–406.
- [74] Toth RA. High resolution measurements and analysis of NO₂ in the (001)–(000) and (011)–(010) bands. *J Opt Soc Amer* 1992;B9:433–61.
- [75] Malathy Devi, V, Fridovitch B, Jones GD, Snyder GD, Das PP, Flaud J-M, Camy-Peyret C, Narahari Rao K, Tunable diode laser spectroscopy of NO₂ at 6.2 μm —Self and N₂-broadenings. *J Mol Spectrosc*, 1982;93:179–95.
- [76] Kleiner I, Tarrago G, Brown LR. Analysis of $3\nu_2$ and $\nu_2 + \nu_4$ of ¹⁴NH₃ near 4 μm . *J Mol Spectrosc* 1995;173:120–45.
- [77] Guelachvili G, Abdulah A, Tu N, Narahari Rao K, Urban S, Papousek D. Analysis of high-resolution Fourier-transform spectra ¹⁴NH₃ at 3.0 μm . *J Mol Spectrosc* 1989;133:345–64.
- [78] Urban S, Tu N, Narahari Rao K, Guelachvili G. Analysis of high-resolution Fourier-transform spectra ¹⁴NH₃ at 2.3 μm . *J Mol Spectrosc* 1989;133:312–30.
- [79] Brown, LR, Margolis JS. Empirical line parameters of NH₃ from 4791–5294 cm^{-1} . *J Quantitative Spectrosc Radiative Transfer* 1996;56:283–94.
- [80] Urban S, Pracna P. Private communication 1993.
- [81] Pine AS, Dang-Nhu M. Spectral intensities in the ν_1 band of NH₃. *J Quantitative Spectrosc Radiative Transfer* 1993;50:565–70.
- [82] Margolis JS, Kwan YY. The measurement of the absorption strength of some lines in the $\nu_1 + \nu_3$ and $\nu_2 + \nu_3$ bands of ammonia. *J Mol Spectrosc* 1974;50:266–80.
- [83] Kleiner I, Tarrago G, Brown LR, Kou Q-L, Pique N, Guelachvili G, Dana V, Mandin J-Y. Positions and intensities in the $2\nu_4/\nu_1/\nu_3$ vibrational system of ¹⁴NH₃ near 3 μm . *J Mol Spectrosc* (submitted).
- [84] Pine AS, Markov VN, Buffa G, Tarrini O, N₂, O₂, H₂, Ar and He broadening in the ν_1 band of NH₃. *J Quantitative Spectrosc Radiative Transfer* 1993;50:337–48.
- [85] Markov VN, Pine AS, Buffa G, Tarrini O. Self-broadening in the ν_1 band of NH₃. *J Quantitative Spectrosc Radiative Transfer*, 1993;50:167–78.

- [86] Brown LR, Plymate C, H₂-broadened H₂¹⁶O in four infrared bands between 55 and 4045 cm⁻¹. *J Quantitative Spectrosc Radiative Transfer* 1996;56:263–82.
- [87] Goldman A, Rinsland CP, Perrin A, Flaud J-M. HNO₃ line parameters: 1996 HITRAN update and new results. *J Quantitative Spectrosc Radiative Transfer* 1998;60:851–61.
- [88] Perrin A, Jaouen V, Valentin A, Flaud J-M, Camy-Peyret, C. The ν_5 and $2\nu_9$ bands of nitric acid. *J Mol Spectrosc* 1993;157:112–21.
- [89] Perrin A, Flaud J-M, Camy-Peyret C, Jaouen V, Farrenq R, Guelachvili G, Kou Q, Le Roy F, Morillon-Chapey M, Orphal J, Badaoui M, Mandin J-Y, Dana V. Line intensities in the 11 and 7.6 μm bands of HNO₃. *J Mol Spectrosc* 1993;160:524–39.
- [90] Goldman A, Rinsland CP, Murcray FJ, Blatherwick RD, Murcray DG. High resolution studies of heavy NO_y molecules in atmospheric spectra. *J Quantitative Spectrosc Radiative Transfer* 1994;52:367–77.
- [91] Giver LP, Valero FPJ, Goorvitch D, Bonomo FS. Nitric-acid band intensities and band-model parameters from 610 to 1760 cm⁻¹. *J Opt Soc Amer* 1984;B1:715–822.
- [92] Perrin A, Flaud J-M, Camy-Peyret C, Winnerwisser BP, Klee S, Goldman A, Murcray FJ, Blatherwick RD, Bonomo FS, Murcray DG, Rinsland CP. First analysis of the $3\nu_9 - \nu_9$, $3\nu_9 - \nu_5$ and $3\nu_9 - 2\nu_9$ bands of HNO₃: torsional splitting in the ν_9 vibrational mode. *J Mol Spectrosc*, 1994;166:224–43.
- [93] Goldman A, Perrin A, Rinsland CP. Private communication, 1997.
- [94] Goldman A, Rinsland CP. HNO₃ line parameters: new results and comparisons of simulations with high-resolution laboratory and atmospheric spectra. *J Quantitative Spectrosc Radiative Transfer* 1992;48:653–66.
- [95] May RD, Webster CR. Measurements of line positions, intensities, and collisional air-broadening coefficients in the HNO₃ 7.5 μm band using a computer controlled tunable diode laser spectrometer. *J Mol Spectrosc* 1989;138:383–97.
- [96] Coxon JA, Foster SC. Rotational analysis of hydroxyl vibration-rotation emission bands: molecular constants for OH X² Π , $6 \leq v \leq 10$. *Can J Phys*, 1982;60:41–8.
- [97] Abrams MC, Davis SP, Rao MLP, Engleman R, Jr Brault JW. High-resolution Fourier transform spectroscopy of the Meinel system of OH. *Astrophys J Suppl Ser* 1994;93:351–95.
- [98] Melen F, Sauval AJ, Grevesse N, Farmer CB, Servais Ch, Delbouille L, Roland G. A new analysis of the OH radical spectrum from solar infrared observations. *J Mol Spectrosc* 1995;174:490–509.
- [99] Goorvitch D, Galant DC. Schrödinger's radial equation solution by extrapolation. *J Quantitative Spectrosc Radiative Transfer* 1992;47:391–9; Goorvitch D, Galant DC. The solution of coupled Schrödinger equations using an extrapolation method. *J Quantitative Spectrosc Radiative Transfer* 1992;47:505–13; Goorvitch D, Goldman A, Dothe H, Tipping RH, Chackerian C, Jr, Hydroxyl X² Π pure rotational transitions. *J Geophys Res* 1992;97:20771–86; Chackerian C, Jr, Goorvitch D, Benidar A, Farrenq R, Guelachvili G, Martin PM, Abrams MC, Davis SP. Rovibrational intensities and electric dipole moment function of the X² Π hydroxyl radical. *J Quantitative Spectrosc Radiative Transfer* 1992;48:667–73.
- [100] Nelson DD, Jr, Schiffman A, Nesbitt DJ, Orlando JJ, Burkholder JB. H + O₃ Fourier-transform infrared emission and laser absorption studies of OH(X² Π) radical: an experimental dipole moment function and state-to-state Einstein A coefficients. *J Chem Phys* 1990;93:7003–19; Chackerian C, Jr, Goorvitch D, Benidar AA, Farrenq R, Guelachvili G, Abrams MC, Davis SP. Private communication, 1997.
- [101] Rothman LS, Gamache RR, Goldman A, Brown LR, Toth RA, Pickett HM, Poynter RL, Flaud J-M, Camy-Peyret C, Barbe A, Husson N, Rinsland CP, Smith MAH. The HITRAN database: 1986 edition. *Appl Opt* 1987;26:4058–97.
- [102] Bastard D, Bretenoux A, Charru A, Picherit F. Determination of mean collision cross-sections of free radical OH with foreign gases. *J Quantitative Spectrosc Radiative Transfer* 1979;21:369–2.
- [103] Chance KV, Jennings DA, Evenson KM, Vanek MD, Nolt IG, Radostitz JV, Park K. Pressure broadening of the 118.455 cm⁻¹ rotational lines of OH by H₂, He, N₂, and O₂. *J Mol Spectrosc*, 1991;146:375–80.
- [104] Schiffman A, Nesbitt DJ. Pressure broadening and collisional narrowing in OH ($v = 10$) rovibrational transitions with Ar, He, O₂, and N₂. *J Chem Phys* 1994;100:2677–89.
- [105] Park K, Zink LR, Evenson KM, Chance KV, Nolt IG. Pressure broadening of the 83.869 cm⁻¹ rotational lines of OH by N₂, O₂, H₂ and He. *J Quantitative Spectrosc Radiative Transfer* 1996;55:285–7.

- [106] Buffa G, Tarrini O, Inguscio M. Prediction for collisional broadening of far-infrared OH rotational lines of atmospheric interest. *Appl Opt* 1987;26:3066–8.
- [107] Goldman A, Gillis JR, Rinsland CP, Burkholder JB. Improved line parameters for the X ²Π– X ²Π (1-0) bands of ³⁵ClO and ³⁷ClO. *J Quantitative Spectrosc Radiative Transfer* 1994;52:357–9.
- [108] Burkholder JD, Hammer PD, Howard CJ, Maki AG, Thompson G, Chackerian C. Jr. Infrared measurements of the ClO radical. *J Mol Spectrosc*, 1987;124:139–1.
- [109] Burkholder JD, Hammer PD, Howard CJ, Goldman A. Infrared line intensity measurements in the v = 0-1 band of the ClO radical. *J Geophys Res* 1989;94:2225–34.
- [110] Rinsland CP, Goldman A. Search for infrared absorption lines of atmospheric chlorine monoxide (ClO). *J Quantitative Spectrosc Radiative Transfer* 1992;48:685–92.
- [111] Birk M, Wagner G. Experimental line strengths of the ClO fundamental. *J Mol Spectrosc*, 1997. (submitted).
- [112] Poynter RL, Pickett HM. Submillimeter, millimeter, and microwave spectral line catalog. *Appl Opt*, 1985;24:2235–40.
- [113] Pickett HM, Poynter RL, Cohen EA, Delitsky ML, Pearson JC, Müller HSP. Submillimeter, millimeter, and microwave spectral line catalogue, JPL Publication 80–23, Rev. 4, California Institute of Technology, Pasadena, 1996.
- [114] Waters MW, Reed WG, Froidevaux L, Lungu TA, Peran VS, Stachnik RA, Jarnot RF, Cofield RE, Fishbein EF, Flower DA, Burke JR, Hardy JC, Nakamura LL, Ridenoure BP, Shippony Z, Thurstans RP, Avallone LM, Toohey DW, de Zafra RL, and Shindell DT. Validation of UARS microwave limb sounder ClO measurements. *J Geophys Res* 1996;101:10091–27.
- [115] Oh JJ, Cohen EA. Pressure broadening of ClO by N₂ and O₂ near 204 and 649 GHz and new frequency measurements between 632 and 725 GHz. *J Quantitative Spectrosc Radiative Transfer* 1994;52:151–6.
- [116] Fayt A, Vandenhoute R, Lahaye JG. Global rovibrational analysis of carbonyl sulfide. *J Mol Spectrosc*, 1986;119:233–66.
- [117] Lahaye JG, Vandenhoute R, Fayt A. CO₂ laser saturation Stark spectra and global Stark analysis of carbonyl sulfide. *J Mol Spectrosc* 1986;119:267–79.
- [118] Masukidi, LS, Lahaye JG, Fayt A. Intracavity CO laser Stark spectroscopy of the ν₃ band of carbonyl sulfide. *J Mol Spectrosc*, 1991;148:281–302.
- [119] Grabow J-U, Heineking N, Stahl W. A molecular beam microwave Fourier transform (MB-MWFT) spectrometer with an electric discharge nozzle. *Z Naturforsch* 1991;A46:914–6.
- [120] Maki AG, Wells JS, Burkholder JB. High-resolution measurements of the bands of carbonyl sulfide between 2510 and 3150 cm⁻¹. *J Mol Spectrosc* 1991;147:173–81.
- [121] Horneman V-M, Koivusaari M, Tolonen A-M, Alanko S, Antilla R, Paso R, Ahonen T, Updating OCS 2ν₂ band for calibration purposes. *J Mol Spectrosc* 1992;155:298–306.
- [122] Masukidi LS, Lahaye JG, Fayt A. Intracavity CO and CO₂ laser Stark spectroscopy of the isotopomers of carbonyl sulfide. *J Mol Spectrosc* 1992;154:137–162.
- [123] Dax A, Mürtz M, Wells JS, Schneider M, Bachem E, Urban W, Maki AG. Extension of heterodyne frequency measurements on OCS to 87 THz (2900 cm⁻¹). *J Mol Spectrosc* 1992;156:98–103.
- [124] George T, Wappelhorst MH, Saupe S, Mürtz M, Urban W, Maki AG. Sub-Doppler heterodyne frequency measurements of carbonyl sulfide transitions between 56 and 62 THz. *J Mol Spectrosc* 1994;167:419–28.
- [125] Dax A, Wells JS, Hollberg L, Maki AG, Urban W. Sub-Doppler frequency measurements on OCS at 87 THz (3.4 μm) with the CO overtone laser. *J Mol Spectrosc* 1994;168:416–28.
- [126] Belafhal A, Fayt A, Guelachvili G. Fourier transform spectroscopy of carbonyl sulfide from 1800 to 3120 cm⁻¹: the normal species. *J Mol Spectrosc* 1995;174:1–9.
- [127] Belafhal A, Fayt A, Guelachvili G. Fourier transform spectroscopy of carbonyl sulfide from 1800 to 3120 cm⁻¹: the isotopomers. Private communication, 1997.
- [128] Wells JS, Dax A, Hollberg L, Maki AG, Sub-Doppler frequency measurements on OCS near 1689 and 1885 cm⁻¹. *J Mol Spectrosc* 1995;170:75–81.
- [129] Saupe S, Wappelhorst MH, Meyer B, Urban W, Maki AG. Sub-Doppler heterodyne frequency measurements near 5 μm with a CO-laser sideband system: improved calibration tables for carbonyl sulfide transitions. *J Mol Spectrosc* 1996;175:190–7.

- [130] Fichoux H, Rusinek E, Khelkal M, Legrand J, Herlemont F, Fayt A. Saturation sideband CO₂ laser spectroscopy of the overtone band $2\nu_2$ and its hot band $3\nu_2 - \nu_2$ of carbonyl sulfide. *J Mol Spectrosc* 1998;(in press).
- [131] Hornberger Ch, Boor B, Stuber R, Demtröder W, Naïm S, Fayt A. Sensitive overtone spectroscopy of carbonyl sulfide between 6130 and 6650 cm⁻¹ and at 12000 cm⁻¹. *J Mol Spectrosc* 1996;179:237–45.
- [132] Kagann RH. Infrared absorption intensities for OCS. *J Mol Spectrosc* 1982;94:192–8.
- [133] Dang-Nhu M, Guelachvili G. Intensités des raies d'absorption dans la bande $\nu_2 + \nu_3$ de ¹⁶O¹²C³²S. *Mol Phys* 1986;58:535–40.
- [134] Bouanich J-P, Blanquet G, Walrand J, and Courtoy CP. Diode laser measurements of line strengths and collisional half-widths in the ν_1 band of OCS at 298 and 200 K. *J Quantitative Spectrosc and Radiative Transfer* 1986;36:295–306.
- [135] Blanquet G, Coupe P, Derie F, Walrand J, Spectral intensities in the $2\nu_2^0$ band of carbonyl sulfide. *J Mol Spectrosc* 1991;147:543–5.
- [136] Errera Q, Vander Auwera J, Belafhal A, Fayt A. Absolute intensities in ¹⁶O¹²C³²S: the 2500–3100 cm⁻¹ region. *J Mol Spectrosc* 1995;173:347–69.
- [137] Brown LR. Private communication, 1997.
- [138] Strugariu T, Naïm S, Fayt A, Bredohl H, Blavier J-F, Dubois I. Fourier transform spectroscopy of ¹⁸O-enriched carbonyl sulfide from 1825 to 2700 cm⁻¹. *J Mol Spectrosc* 1998 (in press).
- [139] Bermejo D, Domenech JL, Santos J, Bouanich J-P, Blanquet G. Absolute line intensities in the $2\nu_3$ band of ¹⁶O¹²C³²S. *J Mol Spectrosc* 1997;185:26–30.
- [140] Mouchet A, Blanquet G, Herbin P, Walrand J, Courtoy CP, Bouanich J-P. Diode-Laser Measurements of N₂ broadened line widths in the ν_1 band of OCS. *Can J Phys*, 1985;63:527–31.
- [141] Bouanich J-P, Walrand J, Alberty S, Blanquet G, Diode-Laser Measurements of oxygen-broadened line widths in the ν_1 band of OCS. *J Mol Spectrosc*, 1987;123:37–47.
- [142] Wiedemann G, Bjoraker GL, Jennings DE. Detection of ¹³C-ethane in Jupiter's atmosphere. *Astrophys J* 1991;383:L29-32.
- [143] Orton GS, Lacy JH, Achtermann JM, Parmar P, Blass WE, Thermal spectroscopy of Neptune: the stratospheric temperature, hydrocarbon abundances and isotopic ratios. *Icarus* 1992;100:541–55.
- [144] Kurtz J, Reuter DC, Jennings DE, Hillman JJ. Laboratory spectra of ¹³C-ethane. *J Geophys Res* 1992;96:17489–92.
- [145] Weber M, Blass WE, Reuter DC, Jennings DE, Hillman JJ. The ground state of ¹³C¹²CH₆ (ethane) derived from ν_{12} at 12.2 μm . *J Mol Spectrosc* 1993;159:388–94.
- [146] Weber M, Reuter DC, Sirota JM, Blass WE, Hillman JJ. Fourier transform infrared and tunable diode laser spectra of the ¹³C¹²CH₆ ν_{12} torsion-vibration-rotation band: frequencies, intensities, and barriers to internal rotation. *J Chem Phys* 1994;100:8681–8.
- [147] Weber M, Reuter DC, Sirota JM. A spectral atlas of the ν_{12} fundamental of ¹³C¹²CH₆ in the 12 μm region. NASA Technical Memorandum 104601, Greenbelt, 1994.
- [148] Nikitin A, Champion JP, Tyuterev VI G, Brown LR. The high resolution infrared spectrum of CH₃D in the region 900–1700 cm⁻¹. *J Mol Spectrosc* 1997;184:120–8.
- [149] Nikitin A, Champion JP, Tyuterev VI G, Brown LR, Klee S, Mellau G, Lock M. New assignments of hot band transitions of CH₃D in the region 900–1700 cm⁻¹ and recent results on the analysis of the IR absorption spectrum in the region 1900–3200 cm⁻¹. 15 Colloquium on High Resolution Spectroscopy, Glasgow, 1997.
- [150] Weber M, Blass WE, Halsey GW, Hillman JJ, Maguire WC. l-resonance effects in the ν_5 , $2\nu_5 \leftarrow \nu_5$, and $\nu_4 + \nu_5 \leftarrow \nu_4$ bands of C₂H₂ and ¹³C¹²CH₂ near 13.7 μm . *Spectrochim Acta* 1992;A48:1203–26.
- [151] Weber M, Blass WE, Nadler S, Halsey GW, Maguire WC, Hillman JJ. l-resonance effects in C₂H₂ near 13.7 μm . Part II: The two quantum hot bands. *Spectrochim Acta* 1993;A49A:1659–81.
- [152] Weber M, Blass WE, Halsey GW, Hillman JJ. l-resonance perturbation of IR intensities in ¹²C₂H₂ near 13.7 μm . *J Mol Spectrosc* 1994;165:107–123.
- [153] Lambeau Ch, Fayt A, Duncan JL, Nakagawa T. The absorption of ethylene in the 10 μm region. *J Mol Spectrosc* 1980;81:227–247.
- [154] Cauuet I, Walrand J, Blanquet G, Valentin A, Henry L, Lambeau Ch, De Vleeschouwer M, Fayt A. Extension to third-order Coriolis terms of the analysis of ν_{10} , ν_7 , and ν_4 levels of ethylene on the basis of Fourier transform and diode laser spectra. *J Mol Spectrosc* 1990;139:191–214.

- [155] Legrand J, Azizi M, Herlemont F, Fayt A. Saturation spectroscopy of C₂H₄ using a CO₂ laser sideband spectrometer. *J Mol Spectrosc* 1995;171:13–21.
- [156] Rusinek E, Fichoux H, Khelkhal M, Herlemont F, Legrand J, Fayt A. Sub-Doppler study of the ν_7 band of C₂H₄ with a CO₂ laser sideband spectrometer. *J Mol Spectrosc* 1998 (in press).
- [157] Herlemont F, Lyszyk M, Lemaire J, Lambeau Ch, De Vleeschouwer M, Fayt, A. Saturated absorption of C₂H₄ with a CO₂ waveguide laser. *J Mol Spectrosc* 1982;94:309–15.
- [158] Blass WE, Jennings L, Ewing AC, Daunt SJ, Weber MC, Senesac L, Hager S, Hillman JJ, Reuter DC, Sirota JM, *J Quantitative Spectrosc Radiative Transfer* 1998 (in press).
- [159] Brannon JF, Varanasi P, Tunable Diode-Laser measurements on the 951.7393 cm⁻¹ line of C₂H₄-¹²C at planetary atmospheric temperatures. *J Quantitative Spectrosc Radiative Transfer*, 1992;47:237–242; Brannon JF, Varanasi P, Tunable Diode-Laser measurements on the 951.7393 cm⁻¹ line of C₂H₄-¹²C at planetary atmospheric temperatures. *J Quantitative Spectrosc Radiative Transfer*, 1993;6:695–6.
- [160] Pine AS. Tunable laser survey of molecular air pollutants, Final Report, NSF/ASRA/DAR 78-24562, MIT, Lexington, MA. 1980.
- [161] Mellau G, Klee S. Unpublished results, 1997.
- [162] Fayt A, Gulaczyk I, Oomens J, Reuss J, Sartakov B, Mellau G, Klee S. Cold and hot bands of ethylene in the 3000 cm⁻¹ region, Proc. 14th Int Conf on High Resolution Molecular Spectroscopy, Prague, Czech Republic, September 9–13 1996.
- [163] Sartakov BG, Oomens J, Reuss J, Fayt A. Interaction of vibrational fundamental and combination states of ethylene in the 3 μ m region. *J Mol Spectrosc* 1997;185:31–47.
- [164] Dang-Nhu M, Pine AS, Fayt A, De Vleeschouwer M, Lambeau Ch. Les intensités dans la pentade ν_{11} , $\nu_2 + \nu_{12}$, $2\nu_{10} + \nu_{12}$, ν_9 et $\nu_3 + \nu_8 + \nu_{10}$ de ¹²C₂H₄. *Can J Phys* 1983;61:514–21.
- [165] Herzberg G, Molecular spectra and molecular structure. vol. 2. Infrared and Raman spectra of polyatomic molecules. New York: D. Van Nostrand Company, 1945;325–8.
- [166] Chance K, Jucks KW, Johnson DG, Traub WA. The Smithsonian astrophysical observatory database. *J Quantitative Spectrosc Radiative Transfer* 1994;52:447–58.
- [167] Flaud J-M, Camy-Peyret C, Johns JWC, Carli B. The far infrared spectrum of H₂O₂: first observation of the staggering of the levels and determination of the cis barrier. *J Chem Phys* 1989;91:1504–10.
- [168] Camy-Peyret C, Flaud J-M, Johns JWC, Noel M. Torsion–vibration interaction in H₂O₂: first high resolution observation of ν_3 . *J Mol Spectrosc* 1992;155:84–104.
- [169] Perrin A, Flaud J-M, Camy-Peyret C, Schermaul R, Winnewisser M, Mandin J-Y, Dana V, Badaoui M, Koput J. Line intensities in the far infrared spectrum of H₂O₂. *J Mol Spectrosc* 1996;176:287–96.
- [170] Malathy Devi V, Rinsland CP, Smith MAH, Benner DC, Fridovitch B, Tunable diode laser measurements of air-broadened linewidths in the ν_6 band of H₂O₂. *Appl Opt* 1986;25:1844–7.
- [171] Brown LR, Crisp J, Crisp D, Naumenko OV, Smirnov MA, Sinita LN. The absorption spectrum of H₂S between 2150 and 4260 cm⁻¹. *J Mol Spectrosc*, 1998;187 (in press).
- [172] Bykov AD, Naumenko OV, Smirnov MA, Sinita LN, Brown LR, Crisp J, Crisp D. The infrared spectrum of H₂S from 1 to 5 μ m. *Can J Phys* 1994;72:989–1000.
- [173] Waschull J, Kuhnemann F, Sumpf B, Self-broadening air, and helium broadening in the ν_2 band of H₂S. *J Mol Spectrosc* 1994;165:150–8.
- [174] Meusel I, Sumpf B, Kronfeldt HD. Nitrogen broadening of absorption lines in the ν_1 , ν_2 , and ν_3 bands of H₂S determined applying an IR diode-laser spectrometer. *J Mol Spectrosc* 1997;185:370–373.
- [175] Ballard J, Johnston WB, Gunson MR, Wassell PT, Absolute absorption coefficients of ClONO₂ infrared bands at stratospheric temperatures. *J Geophys Res*, 1988;93:1659–65.
- [176] Massie ST, Goldman A. Absorption parameters of very dense molecular spectra for the HITRAN compilation. *J Quantitative Spectrosc Radiative Transfer* 1992;48:713–9.
- [177] Goldman A, Rinsland CP, Murcray FJ, Blatherwick RD, Murcray, DG. High resolution studies of heavy NO_y molecules in atmospheric spectra. *J Quantitative Spectrosc Radiative Transfer* 1994; 52:367–77.
- [178] Bell W, Duxbury G, Stuart DD. High-resolution spectra of the ν_4 band of chlorine nitrate. *J Mol Spectrosc* 1992;152:283–97.

- [179] Rinsland CP, Gunson MR, Abrams MC, Zander R, Mahieu E, Goldman A, Ko MKW, Rodriguez JM, Sze ND. Profiles of stratospheric chlorine nitrate (ClONO₂) from atmospheric trace molecule spectroscopy/ATLAS 1 infrared solar occultation spectra. *J Geophys Res* 1994;99:18895–900.
- [180] Goldman A, Rinsland CP, Flaud J-M, Orphal J. ClONO₂: spectroscopic line parameters and cross-sections in 1996 HITRAN. *J Quantitative Spectrosc Radiative Transfer* 1998;60:875–82.
- [181] Rogers JD, Stefens RD. Absolute infrared intensities for F-113 and F-114 and an assesment of their greenhouse warming potential relative to other chlorofluorocarbons. *J Geophys Res* 1988;93:2423–8.
- [182] World Meteorological Organization (WMO), Atmospheric ozone: assessment of our understanding of the process controlling its present distribution and hange, Rep. 16, 1985, vol. II, Chap. 11, pp. 632–47.
- [183] World Meteorological Organization (WMO), Scientific assessment of ozone depletion. In *Global Ozone Research and Monitoring Project*, Rep. 25, Geneva, Switzerland, 1991.
- [184] Ramanathan V, Cicerone RJ, Singh HB, Kiehl JT. Trace gas trends and their potential role in climate change. *J Geophys Res* 1985;93:2423–28.
- [185] Clerbaux C, Colin R, Simon PC, Granier C. Infrared cross-sections and global warming potentials of 10 alternative hydrohalocarbons. *J Geophys Res*, 1993;98(D6):10491–7.
- [186] Massie ST, Goldman A, McDaniel AH, Cantrell CA, Davidson JA, Shetter RE, Calvert JG. Temperature dependent infrared cross sections for CFC-11, CFC-12, CFC-13, CFC-14, CFC-22, CFC-113, CFC-114, and FC-115. NCAR. Technical Note TN-358 + STR, 1991.
- [187] McDaniel AH, Cantrell CA, Davidson JA, Shetter RE, Calvert JG, The temperature dependent infrared cross sections for CFC-11, CFC-12, CFC-13, CFC-14, CFC-22, CFC-113, CFC-114, and CFC-115. *J Atmos Chem* 1991;12:211–7.
- [188] Li Z, Varanasi P. Measurement of the absorption cross-sections of CFC-11 at conditions representing various model atmospheres. *J Quantitative Spectrosc Radiative Transfer* 1994;52:137–44.
- [189] Varanasi P, Nemtchinov V. Thermal infrared absorption coefficients of CFC-12 at atmospheric conditions. *J Quantitative Spectrosc Radiative Transfer* 1994;51:679–87.
- [190] Varanasi P, Li Z, Nemtchinov V, Cherukuri A. Spectral absorption coefficient data on HCFC-22 and SF₆ for remote sensing applications. *J Quantitative Spectrosc Radiative Transfer* 1994;52:323–32.
- [191] Smith K, Newnham D, Page M, Ballard J, Duxbury G. Infrared band strengths and absorption cross-sections of HCF-32 vapor. *J Quantitative Spectrosc Radiative Transfer* 1996;56:77–82.
- [192] Smith K, Newnham D, Page M, Ballard J, Duxbury G. Infrared absorption cross-sections and integrated absorption intensities of HFC-134 and HFC-143a vapour. *J Quantitative Spectrosc and Radiative Transfer* 1998;59:437–51.
- [193] Massie ST, Goldman A, Murcraay DG, Gille JC. Approximate absorption cross-sections of F12, F11, ClONO₂, N₂O₅, HNO₃, CCl₄, CF₄, F21, F113, F114, and HNO₄. *Appl Opt* 1985;24:3426–7.
- [194] Orphal J, Guelachvili G, Morillon-Chapey M. High-resolution absorption cross-sections of chlorine nitrate in the ν₂ band region around 1292 cm⁻¹ at stratospheric temperatures. *J Geophys Res*, 1994;99(D99):14549–55.
- [195] Varanasi P, Nemtchinov V. Private communication, 1998.
- [196] Chursin AA, Golovko VF, Tyuterev VIG, Husson N, Bonnet B, Chedin A, Scott NA. The software package for managing large-scaled spectroscopic databases and its atmospheric applications. In *Proc 2nd Int Workshop on Advances in Databases and Information Systems*, vol. 2, Moscow, Russia, 1995;9–11.
- [197] Chursin AA, Golovko VF, Nikitin AV, Jacquinet-Husson N, Bonnet B, Scott NA, Tyuterev VIG. The GEISA-PC software packages for large-scaled spectroscopic databases management: current status and perspectives. In *Proc 1st East-European Symp on Advances in Databases and Information Systems (ADBIS-97)*, vol. 2, St.-Petersburg, Russia, 1997;70–2.